Works-in-Progress

Abstracts in this section pertain to papers as Works-in-Progress at the 35th Annual Meeting of the SNM, June 14-17, 1987 held at the George Moscone Convention Center, San Francisco, CA. Scientific Program Chairman: Paul H. Murphy, PhD

Bone/Joint

Posterboard 1200

180 DEGREES FACIO-VERTEX-OCCIPITAL BONE SPECT OF SKULL. K.Machida, N.Honda, T.Mamiya, T.Takishima, T.Takahashi, K.Ohno, M.Muramatsu and M.Hosoba*. Saitama Medical Center, Saitama Medical School, Kawagoe and *Shimadzu Corporation, Kyoto, Japan.

In order to save scan time of Tc-99m MDP bone SPECT of skull, we performed 180 degrees facio-vertex-occipital SPECT (FVO) in seven cases with normal and abnormal skull scintigrams. And those SPECT images were compared with conventional 360 degrees transaxial SPECT images. Two or three hours after intravenous administration of 20mCi of Tc-99m MDP, in 180 degrees FVO, data were collected from 32 directions and each image was recorded for 20 seconds, and in 360 degrees conventional SPECT, data were collected from 64 directions and each image was recoreded for 15 seconds.

Three doctors analyzed the quality of SPECT images for each part of skull, that is frontal, parietal, temporal, occipital skull, lateral orbita, skull base, maxilla and mandible. The quality of images was classified into three grades; excellent, good and poor.

It was found that there was no significant difference in the quality of images and in diagnosing abnormal area anatomically. We conclude 180 degrees FVO is useful and could be used clinically for bone SPECT of skull.

Posterboard 1201

QUANTITATIVE SPECT SCANS OF ALLERGIC SINUSITIS. L.D. Samuels, A.P.Zilliox and R.G.Slavin, The University Hosital, St. Louis University, St. Louis, MO.

These studies were undertaken to determine whether demonstratable changes in the bone surrounding the sinuses occur coincident with clinical allergic sinusitis.

Three patients with acute ragweed allergy were studied in the midst of ragweed season. Twenty mCi Tc-99m MDP were injected I.V. and immediate ten minute SPECT imaging of the head was performed. Two hours later SPECT imaging of the head was also performed. Transverse, sagittal and coronal slices 6 mm. thick were obtained and quantitatively analyzed. One patient was restudied six weeks later, after the end of the ragweed season. Subsequently patients with vasomotor rhinitis and grass allergy are under study.

There was hyperemia and increased bone uptake around both maxillary sinuses associated with acute allergic attacks. This was not seen in the patient restudied after the allergy season was past. These findings are a first SPECT documentation of physical change in bone associated with allergic sinusitis.

Posterboard 1202

SAMARIUM-153 EDTMP THERAPY DOSIMETRY AND SPECT IN CANCER PATIENTS WITH DISSEMINATED SKELETAL METASTASIS. J.H. Turner, R.F. Hoffman, A.A. Martindale, E.L. Hetherington, P. Sorby and P.G.Claringbold, Fremantle Hospital Western Australia and Australian Nuclear Science and Technology Organization, NSW, Australia.

The 103 kev gamma emission of Sm-153 was used for quantitative SPECT imaging to determine beta dosimetry in a clinial trial of Sm-153 ethylene diamine tetramethylene phosphonate (EDTMP) therapy for disseminated skeletal metastasis. Tumour to bone uptake ratios of Sm-153 EDTMP from a freeze dried kit formulation were found to be the same as those obtained with Tc99m MDP on SPECT performed the previous week. All metastases evident on the Tc-99m MDP images were demonstrated in Sm-153 EDTMP studies performed on 12 patients with widespread bone metastasis from carcinoma of breast,prostate and lung. Dosimetry calculations on a preliminary administered dose of 10 mCi Sm-153 EDTMP verified that over 55% of Sm-153 administered IV was retained in the skeleton, 98% of non-osseous activity being cleared by urinary excretion within 6 hours. Preferential uptake in bone metastases with tumour to normal bone ratios of greater than 2.5:1 was demonstrated in all patients. From therapy doses of 0.4-0.75 mCi/kg, red marrow exposure was calculated at 50-115 rads. There was no depression of normal leucocyte and platelet counts over 6 weeks following an average dose of 25-50 mCi Sm-153 EDTMP.Calculated tumour irradiation varied between patients and within individual bone metastases in the range 250-1200 rads. Follow-up Tc99m MDP studies at 3 months demonstrated stabilization of metastases in 10 patients. Pain was relieved in all patients. Recurrence of bone pain after 6 weeks in 3 patients responded to re-treatment with Sm-153 EDTMP.

Cardiovascular—Basic

Posterboard 1203

VENTRAL DECUBITUS : THE SOLUTION FOR DIAPHRAGMATIC ATTENUATION IN THALLIUM 201 MYOCARDIAL TOMOGRAPHY. J.P. Esquerré - F.J. Coca - S.J. Martinez - R.F.Guiraud C.H.U. Toulouse Purpan - France

Diaphragmatic attenuation in 201 Tl 180° myocardial SPECT results in reduced specificity in the detection of inferior wall(IW) abnormalities due to possible attenuation artifacts and widening of the standard deviation (SD) of IW maximum counts circumferential profiles (CPs).

To test if ventral decubitus which should result in shifting down diaphragm and subphrenic organs could be a solution to this problem, we systematically performed 201 Tl redistribution SPECT studies in both supine and ventral positions. We compared homologous medioventricular thick short axis slices by visual interpretation and CPs analysis.

Among 25 patients a posteriori considered as normal on the basis of normal stress ECG and coronary arteriography, 17 presented a more or less reduced activity in the IW in the supine study, none of them in the ventral study.

The mean normalized supine CP showed a minimum at 84 % $\pm$ 14 % (1 SD) in the IW. The SD decreased to around 6 % in the antero lateral part of the CP which was nearly flat. The mean normalized ventral CP was horizontal in the limits of statistic fluctuations without no signifi-

cant minimum in the IW and the SD remained almost cons - tant around 6 % along the whole CP.

We conclude that ventral position drastically impro - ves sensitivity and specificity in the evaluation of IW abnormalities by suppressing attenuation artifacts and, by the way, the effects of high individual variability in left phrenic and subphrenic anatomic configuration and stomach degree of repletion.

Posterboard 1204

TRANSPORT OF HEXAKIS (2-METHOXY ISOBUTYLISONITRILE) BY ISOLATE CALCIUM COMPETENT PIG ADULT CARDIAC MYOCYTES.

E.I. Gonzalez, J. Rivera and C.A. Rabito.
Massachusetts General Hospital, Boston, MA.

Hexakis (2-methoxy isobutylisonitrile) 99mTc has been used recently as a myocardial imaging agent as an alternative to Tl-201 in the diagnosis of ischemic heart disease. Although this agent has shown favorable characteristics as a Tl-201 substitute, there are fundamental questions about the basic mechanisms of tissue localization that still remain unanswered or at least controversial. In order to understand these mechanisms, we studied the influx of MII-Tc and Tl-201 in isolated calcium competent, pig adult cardiac myocytes. Seven to 10 day old pigs were anesthetized with inactin and the heart removed and placed in cold saline. After that, the heart was placed in a Langendorff perfusion system and perfused with NCTC-135 culture medium at 37°C. After 15 minutes, the NTC-135 culture medium was replaced by Ca^{2+} and Mg^{2+}-free minimal essential medium (MEM). After 5 minutes, the perfusion medium was replaced again by MEM containing 50uM Ca^{2+}, 2 mg/ml collagenase, 2.5mg/ml hyaluronidase and 0.1% bovine serum albumin. The perfusion was continued for another 15 minutes. The heart was removed from the perfusion system and placed in a 10cm plastic petri dish containing 50uM Ca^{2+} MEM without enzymes. The cells were gently dispersed with a small glass hook and suspended in complete NCTC-135 culture medium. Viability of isolated myocytes ranged from 60 to 90% as determined by the rod shape, contractile activity, oxygen consumption and electrolyte distribution. Incubation of the isolated myocytes in presence of 10^{-3}M ouabain produce a significant inhibition of Tl-201 influx. The uptake of MII-Tc increases with the incubation times to reach steady-state distribution after 30 minute incubation. This uptake was not inhibited when the myocyctes were incubated in presence of 10^{-3}M ouabain. From these results, we conclude that isolated, calcium competent adult cardiac myocytes could be used to study the cellular mechanisms involved in the myocardial accumulation of MII-Tc.

Posterboard 1205

THROMBUS IMAGING WITH I-123 LABELED F(ab'2) FRAGMENT OF A MURINE MONOCLONAL ANTIBODY SPECIFIC FOR HUMAN FIBRIN FRAGMENT D-DIMER IN A RABBIT MODEL OF VENOUS THROMBOSIS.

Y. Hashimoto, J.M. Stassen, B. Leclef, M. DeRoo, A. Vandecruys, J. Melin, C. Waterkeyn, A. Trouet and D. Collen. Center for Thrombosis and Vascular Research, Laboratory of Nuclear Medicine, University of Leuven; Division of Nuclear Medicine, University of Louvain and IRE-Celltarg, BELGIUM.

The F(ab'2) fragment of a murine monoclonal antibody specific for human fibrin fragment D-dimer (MA-15C5) was labeled with I-123 to a specific activity of 20 ± 2 µCi/µg and injected intravenously (20 µg/kg) in 8 rabbits with a non-occlusive 0.2 ml human plasma clot in the jugular vein and in 9 rabbits that underwent surgery but without clot formation. Total body scans were performed hourly for 12 hrs and blood samples were taken to determine the turnover (t1/2= 15 ± 2.8 hrs). The results of gamma-ray emission in the clot region as compared to the symmetrical region and the head region, were:

	Excess gamma counts (% of first scan)					
	vs. symmetrical			vs. head		
Group	1 hr	5 hr	10 hr	1 hr	5 hr	10 hr
Thrombus	10±4	58±17	81±22	9±2	53±14	79±19
Controls	2±3	-2±5	-1±6	6±3	9±5	12±6
p <	0.02	0.005	0.005	0.1	0.01	0.005

In vitro the vein segment to the contralateral vein segment count ratios were 10.6 ± 5.9 in rabbits with clot versus 1.9 ± 0.5 in the controls ($p < 0.005$). All data represent mean ± SEM.

We conclude that this F(ab'2)fragment has a sufficient ly high fibrin affinity to allow in vivo thrombus localisation by external scanning.

Posterboard 1206

Assessment of myocardial perfusion and segmental wall motion with 99mTc-2-methoxy-isobutylisonitrile(MIBI): comparison with radionuclide ventriculography and echocardiography.

F.Mut,E.Besada,A.Beltran,G.Martínez,C.Oliveira,E.Touya. Centro de Medicina Nuclear,Hospital de Clínicas,Montevideo,Uruguay.

To determine the value of 99mTc-2-methoxy-isobutylisonitrile(MIBI)as an agent for myocardial perfusion and wall motion,10 patients with documented myocardial infarction were studied.Each patient underwent a resting SPECT and 3 view(anterior,LAO 45°and left lateral) multigated study starting 60 minutes after intravenous injection of 99mTc-MIBI(25mCi,925MBq),followed 6 days later by a 3-view radionuclide ventriculography and 2-D echocardiography. SPECT studies were reconstructed and reoriented to obtain transaxial,lateral and superior slices.For each imaging method,left ventricular wall was divided into 12 segments and a 3 point scoring system was used for perfusion(2=normal,1=hypokinesis,0=akinesis or dyskinesis).The site of myocardial necrosis was correctly identified by SPECT MIBI in all 10 patients when compared with ECG changes.Mean perfusion score (120 segments)with MIBI was 16.5±1.8, while mean wall motion score was 19.5±1.4 for gated MIBI, 19.1±1.6 for RNV and 19.3±1.7 for ECO(p=NS between any of the last three methods).Segment to segment coincidence in score was 88% between MIBI perfusion and MIBI gated, 92% between MIBI gated and RNV,and 96% between MIBI gated and ECO.

In conclusion,99mTc-MIBI is a reliable agent for both myocardial perfusion and segmental wall motion evaluation

Posterboard 1207

COMPARISON OF Tc-99M SQ 30,217, Tl-201 AND I-123 MIBG IN A DOG MODEL OF MYOCARDIAL DENERVATION.

Wellman H, Tuli M, Weiner R, Stanton M, Zipes D, Beal M, and Pride P. Indiana U. School of Medicine, Indianapolis, IN.

An evaluation of SPECT myocardial imaging (Elscint Apex-415-ECT-LEAP collimator) comparing a new neutral lipophilic perfusion agent, Tc-99m SQ 30,217,* (SQ) with Tl-201 and I-123 MIBG was carried out in two myocardial denervation (MDN) models. Nine dogs had baseline studies with SQ and MIBG. MDN was produced surgically by epicardial phenol application (PA) (n=3) and a small experimental transmural myocardial infarction (tMI) (n=4). Sham operations were performed as control (n=2). Post-op (1-2 wks) studies with all agents were blindly interpreted. All dogs underwent open heart electrophysiological studies (EPS) to verify the status of MDN, followed by sacrifice.

Sham-treated and pre-op images were normal. In the PA group, all SQ and Tl images were normal, as expected. In 2 dogs, defects were observed with MIBG and EPS confirmed MDN. The 3rd dog's MIBG image was normal as was EPS, thus an unsuccessful surgical MDN. Two dogs with tMI had lesions identified by all agents and MDN was confirmed at EPS. As anticipated from our previous work, lesions observed with MIBG were more extensive than with either Tl or SQ. Images of the other 2 tMI dogs were normal with all agents. The EPS was normal in one and equivocal in the other, both had a tMI at postmortem. Planar image quality with SQ was superior to Tl, however, SPECT quality of both was similar. In these 2 models of MDN, SQ was as good as or better than Tl and having the advantages of the Tc-99m label, such as rapid SPECT acquisition and ready availability.

*Squibb Diagnostics

Cardiovascular—Clinical

Posterboard 1208

SILENT VERSUS CHEST PAIN ASSOCIATED MYOCARDIAL PERFUSION CHANGES IN EXERCISE THALLIUM-201 SPECT IMAGES OF PATIENTS WITH CORONARY ARTERY DISEASE. M. Ahmad, H.D. Fawcett, and M.L. Nusynowitz. The University of Texas Medical Branch at Galveston, Tx.

To assess the significance of silent myocardial perfusion changes during exercise in patients with coronary artery disease (CAD), we studied 59 patients (pts) with angiographically documented CAD, normal resting left ventricular (LV) function and exercise induced thallium-201 (Tl-201) perfusion deficits. Tl-201 perfusion changes during exercise were accompanied by angina in 27 pts (A) and were silent in 32 pts (S). Mean age, previous myocardial infarction, cardiac medications, LV ejection fraction, systolic BP x HR product and number of exercise Tl-201 perfusion deficits were not significantly different between A and S. Eighteen A pts had significant ST↓ during exercise compared to 10 S pts ($p<0.05$); 16 A pts had 3 vessel CAD compared to 10 S pts ($p<0.05$). All pts survived the followup period of one year; complications and treatment were:

Pts/#	Unstable Angina	Myocardial Infarction	Coronary bypass/ Angioplasty
A/27	9	8	14
S/32	4	3	3
p	<0.05	<0.05	<0.003

The data indicate that when exercise induces both angina and Tl-201 perfusion deficits, 3 vessel CAD is more common and complications and surgical intervention more frequent. However, pts with silent Tl-201 perfusion deficits do not necessarily have a benign course.

Posterboard 1209

99MTC HMPAO LABELED PLATELETS (PLT) FOR DEEP VEIN THROMBOSIS (DVT) DIAGNOSIS
P. Bourgeois, M. Stegen, G. Demonceau, W. Feremans, and J.P. Vangysel (CHJ Bracops, Free University of Brussels and Cyclotron Research Unit, University of Liege)

Results of the scintigraphic research of DVT performed 4 to 6 hours and/or 20 to 24 hours after injection of 8 to 12 millicuries of PLT in 18 patients with scintigraphically suspected or proven lung embol (LE) or with clinically suspected or "obvious" DVT have been compared to X Ray phlebography (Phlebo) data.

-Phlebo/PLT	+	-	Tot.
+	10	4••	14 (•••)
-	4•	2	6
Tot.	14	6	20•••

• one case with superficial phlebitis
•• one case with an old thrombus, another one with a marginating one, the two last ones had bilateral thrombi (one side being positive, the heterolateral being negative)
•••two patients with bilateral DVT.

-Precise comparison between Phlebo and PLT pictures demonstrated that PLT delineate only "floating" (fresh) thrombi but, in no case, organized ones

It is concluded that 99mTc HMPAO labeled platelets may represent a sensitive way to diagnose fresh deep vein thrombosis although the methodology up to now developped remains with many false positive conclusions.

Posterboard 1210

MONITORING OF MYOCARDIAL PERFUSION IN ACUTE MYOCARDIAL INFARCTION (AMI) AND THROMBOLYSIS : USEFULNESS OF MIBI-SPECT. M.Faraggi, O.Messian, B.Thonnart, P.Assayag, B.Bok. Hospital Beaujon, Clichy, FRANCE.

Assessing the myocardial perfusion gain with thrombolytic therapy in acute myocardial infarction (AMI) requires perfusion imaging before and after therapy. However, the imaging acquisition time must not delay the immediate thrombolysis. MIBI was administered immediately after admission in 7 patients. Then, if decided, thrombolysis could be done and cardiac imaging was performed 1/2 H later. Because of the absence of redistribution, the pictures still showed the pretreatment MIBI uptake. In one case MIBI SPECT was normal and this patient was considered later as a regressive ischemic event without AMI. In the other six patients with confirmed AMI, the MIBI SPECT was constantly abnormal.

Four patients were seen 1 H 45 to 2 H 30 after the onset of their chest pain and were considered suitable for thrombolytic therapy on the basis of clinical and ECG findings. Then a coronary angiography was performed and MIBI SPECT was repeated after 72 H. Results were : no recovery (1) ; partial recovery (2) ; nearly complete recovery (1). Using this technique, it is then possible to get a high quality myocardial perfusion imaging without delaying treatment of AMI. Our first data suggest that MIBI SPECT may be of interest in showing accurately the size and location of the immediate perfusion defect, and in assessing the response to emergency therapy of AMI, especially thrombolysis.

Posterboard 1211

AN INTERCOMPARISON OF FIRST-PASS TECHNIQUE WITH CARDIAC CATHETERIZATION, DOPPLER AND MUGA FOR EVALUATING LEFT HEART REGURGITATION. J. Mantel, P.N. Cascade, and M. Rubenfire. Sinai Hospital of Detroit, Detroit, MI

The first-pass technique (FP) for measuring regurgitant fraction involves adding the end diastoly counts and end systoly counts of the individual right ventricle and left ventricle beats on the high frequency time-activity curves. The result is an estimate of the right ventricle and left ventricle stroke counts. The ratio of the left ventricle stroke counts to the right ventricle stroke counts is the regurgitant fraction. Sixty-three patients were studied with cardiac catheterization (CC) and FP technique. The degree of regurgitation by CC was evaluated by using a ranking scale of 0-4, where 4 is severe regurgitation. Ten patients with no regurgitation by CC had a percent regurgitation of 3.6±5.5 by FP, five patients with 1-MR had a FP percent regurgitation of 15.8±3.3, thirteen patients with 2-MR had a FP regurgitation of 28.5±14.6, sixteen patients with a 3-MR had a FP regurgitation of 41.5±10.5 and nineteen patients with 4-MR had a FP percent regurgitation of 54.9±13.7. In comparing the ranks, pairwise, we found the averages to be significantly different ($p<.05$). The correlation coefficient between FP and CC for these patients was .90. Twenty-five patients were evaluated with Doppler echocardiography and FP technique for valvular regurgitation. A correlation coefficient of .84 was obtained. Forty-six patients were evaluated for regurgitation by using the blood pool technique (MUGA) and FP. A correlation coefficient of .50 was calculated. We conclude that the FP can quantitate left heart valvular regurgitation. The use of MUGA for this application is not indicated.

Posterboard 1212

COMPARISON OF IMPEDANCE AND NUCLEAR MEDICINE IMAGING DERIVED LEFT VENTRICULAR EJECTION FRACTION. D.S. Miles, R.W. Gotshall, D.W. Wulfeck, J.D. Quinones, R.D. Kreit-

zer, Miami Valley Hospital and Wright State University, Dayton, Ohio.

Preliminary reports have suggested that impedance cardiography may provide another means to noninvasively measure left ventricular ejection fraction (LVEF). The purpose of this study was to compare LVEF as measured by gated radionuclide cardiography (MEF) to that measured from the thoracic impedance cardiogram (ZEF) in both normal subjects and clinically ill patients. The impedance recording was read by four experienced readers to calculate ZEF and the MEF was obtained by two nuclear medicine specialists. Nine subjects, all free of cardiopulmonary disease, were initially studied by the above techniques. The ZEF averaged 0.72 with a range of 0.67 - 0.78 and a coefficient of variation (CV) of 5.9%. The MEF averaged 0.71 (range 0.65 - 0.77) with a CV of 6.1%. Forty-six men and forty-nine women referred for MEF underwent ZEF as well the same day. The mean MEF was 53 $\pm$ 2% while the mean ZEF was 56 $\pm$ 1%. There was no significant difference between the MEF and ZEF for any of the readers. However, correlations between MEF and ZEF were unacceptably low (range -0.17 to 0.16). MEF correlated well with regional wall motion (r=0.84) while ZEF did not (r=0.00). Further analysis, after subdividing the subjects according to regional wall motion failed to improve the correlation with ZEF. These data suggest that the proposed analysis of the impedance cardiogram to measure LVEF should not be used to make a clinical diagnosis and that the radionuclide technique remains superior in evaluating LVEF.

Posterboard 1213

DIAGNOSIS OF CORONARY ARTERY DISEASE BY MYOCARDIAL 201-Tl SPECT COMBINED WITH ATRIAL STIMULATION. L. Nicol, A. Le Helloco, J.Y. Herry. CHU, Pontchaillou, RENNES, FRANCE.

This study aimed at assessing the value of 201-Tl SPECT associated with atrial stimulation (AS) in the detection of coronary artery disease (CAD). 50 patients, 21 with previous myocardial infarction (13 postero-inferior and 8 anterior), 27 with stress or rest angina and 12 with atypical chest pain, underwent AS at increasing frequency and two 201-Tl SPECT investigations, one at the end of stimulation, the other 4 hours later. Selective coronary arteriography, and ECG recordings during AS enabled a diagnosis of CAD to be made in 21 of 39 cases (sensitivity (SE) = 53.8%, specificity = 54.5%). SPECT combined with AS identified defects caused by IVA stenosis of the IVA in 23 of 24 cases (SE = 95.8%), of the right coronary artery in 15 of 16 cases (SE = 93.8%) and of the circumflex artery in 8 of 14 cases (SE = 57%). Overall sensitivity was 89.7% and specificity 81.8%. Our results demonstrate that AS associated with 201-Tl SPECT is a valuable method of diagnosing CAD caused by IVA or right coronary artery stenosis. The method is less efficient in cases of narrowing of the circumflex artery. 201-Tl SPECT combined with AS can be proposed for patients who cannot attain peak stress during exercise testing, for patients with unstable angina and following myocardial infarction.

Posterboard 1214

A NEW SCANNING METHOD FOR THALLIUM-201 MYOCARDIAL EMISSION COMPUTED TOMOGRAPHY:SEMIDECUBITUS POSITION SCANNING METHOD. A. Suzuki, S. Muto*, M. Oshima, H. Saito*, K. Kano, H. Hayashi, Nagoya University School of Medicine, *Tsushima City Hospital, Aichi, Japan.

We designed a new scanning method for thallium-201 myocardial emission computed tomography (ECT) using a rotating gamma camera with 180 degrees data collection. In order to shorten the radial length of gamma camera rotation and to avoid the attenuation of gamma ray by the imaging bed, we manufactured a new bed on which a patient was laid in right semidecubitus (50 degrees) position to make the camera-collimator system close to a patient. Using this method, the radial length of gamma camera rotation was shortened about 25% compared with the conventional imaging system. In addition, the attenuation by the bed was completely avoidable because the projected direction was not overlapped upon the bed during the data acquisition from left posterior oblique views. We have utilized phantom and patient studies for comparison between the conventional and our new scanning method (semidecubitus position scanning method). Using our new method, tomographic images of both phantom and clinical studies showed better resolution and more accumulation of radiotracer in cardiac posteroinferior wall than those by using a conventional scanning method. This result suggests that our new method is useful for thallium-201 myocardial ECT, especially for the evaluation of inferior wall hypoperfusion and dilated cardiomyopathy.

Computers and Data Analysis

Posterboard 1215

DEVELOPMENT OF TOOLS FOR SOFTWARE QUALITY CONTROL (QC). E. Busemann-Sokole, Academic Medical Centre, University of Amsterdam, NL; T.D. Cradduck, University of Western Ontario, London, Canada; J.J. Erickson, Diagnostic Technology Consultants, Fairway, KS.

A common set of patient studies (software phantoms) is necessary for QC of similar applications software from different nuclear medicine computer systems. Incompatible data formats, file contents and magnetic media of the various commercial computers pose the greatest problems in the interchange of software phantoms between computers. Three approaches have been used to overcome this difficulty.

First, a number of real patient data studies have been transferred between systems using hard wired data links. Comparison of the results of applying similar analysis programs to these studies has been reported elsewhere. Second, a mathematical software phantom has been developed that can be applied to any system in which it is possible to program data into a pseudo patient image file. One such mathematical phantom may be used to determine the veracity of Fourier phase and amplitude analysis programs for gated cardiac studies. Because the mathematical phantom provides a standard image pattern, it can also test integrity of data transmission between systems. The third development is to establish a "standard" data file in order to circumvent the difficulties engendered by interchange between different commercial systems. The approach adopted by the AAPM in Report #10 (A Standard Format For Digital Image Exchange) which uses key items has been used as a descriptor to develop a set of key data appropriate to nuclear medicine studies.

Posterboard 1216

REGISTRATION OF PLANAR AND SPECT ABDOMINAL IMAGES WITH MRI AND CT STUDIES FOR MONOCLONAL ANTIBODY STUDIES. G.T.Y. Chen, P. Lee, C.A. Pelizzari, D. Spelbring, and M. Blend*. Michael Reese/University of Chicago Center for Radiation Therapy, and Department of Radiology, *Michael Reese Hospital, Chicago, IL.

Radiolabeled monoclonal antibodies and other biologically specific compounds are under study to

determine their potential in the diagnosis and treatment of human malignancies. The interpretation of the biodistributions obtained from planar and SPECT imaging studies may be improved if they can be directly compared with anatomic information contained in CT and MRI studies. We are studying image correlation techniques for these modalities. For registration of planar scintigraphs, fiducial markers placed on bony landmarks are used to provide coordinate transformations. Anatomical information from CT or MRI are contoured on the axial slices and projected onto a digitally reconstructed radiograph (DRR) generated from the CT/MRI study. The spatially registered radionuclide distribution is overlayed onto the DRR through a color wash technique. A similar approach is used for SPECT studies. An evaluation of the registration techniques is made for both phantom and patient studies. Positional variability of internal organs in the abdomen and pelvis is estimated from serial CT studies.

Posterboard 1217

REGION OF INTEREST ANALYSIS OF SPECT BRAIN IMAGES USING MRI IMAGES AS A STRUCTURAL CORRELATE FOR DETECTION OF HIV DEMENTIA. G.J. Harris, G. Pearlson, N. LaFrance, N.C. Yang, P.Leichner, A.J. Kumar, M.J. Bascom, J.A. Mendizabel. The Johns Hopkins Medical Institutions, Baltimore, MD.

Human Immunodeficiency Virus (HIV) invades the central nervous system in many of those infected. There, the virus attacks brain cells and produces HIV dementia in perhaps two-thirds of those who possess the virus. The goal of this project is the observation of regional cerebral blood flow alteration using [I-123]-N-isopropyl Iodoamphetamine (IMP, Spectamine) in patients with HIV infection. The program described below enables the definition of subcortical regions, and observation of their blood flow, which would be difficult using single photon emission computed tomography (SPECT) alone.

A program was developed to enable the extraction of region of interest information from SPECT brain images using a magnetic resonance imaging (MRI) image as an anatomical marker. An edge follower boundary search was used to define the boundary of the structure of interest from the MRI image slice. The SPECT slice is then determined for the corresponding depth of the slice. The SPECT slice is aligned in the same rotational frame as the MRI slice. An adjustment is then made to account for differences between the cartesian coordinates of the centers of the two brain images, and differing pixel sizes in the images. The program allows automatic boundary position and size adjustment, or a manual repositioning and size shift. This allows the user to observe any size and position region which may be of interest. The area of the region and the average pixel value within the region are supplied by the program.

Posterboard 1218

CT/SPECT FUSION FOR CORRELATION OF MONOCLONAL ANTIBODY (MOAB) SPECT AND ABDOMINAL CT. EL Kramer, ME Noz, JJ Sanger, GQ Maguire and A Megibow, NYU Medical Center/Bellevue Hospital Center and Columbia University.

Although radiolabeled MoAb SPECT studies provide tissue specific information, they are deficient in anatomic landmarks. We have developed a technique for closely aligning abdominal SPECT slices with CT in order to enhance the information from both modalities.

SPECT studies of patients with suspected colorectal carcinoma were performed 3-7 days after administration of 5 mCi of an In-111 labeled anti-CEA MoAb (Hybritech, Inc.). 2 SPECT acquisitions were performed: one with external Co-57 markers placed at 4-5 external anatomic sites chosen for their easy correlation with identifiable landmarks on the CT, the other with the markers removed and the energy windows readjusted for In-111 (173, 247 keV). After uniformity and center-of-rotation correction are applied, filtered backprojection is performed on the entire volume of both sets of projections to reconstruct one pixel-thick (~6.3.mm) slices. 10 mm CT slices were obtained at 12 mm intervals from diaphragm to anus.

SPECT and CT slices are transferred to a SUN 380 Workstation/ PIXAR Image Computer. CT and SPECT images are interpolated to a common matrix size. Marker and MoAb SPECT slices are added together and merged into 2-pixel thick slices to match the CT slice thickness. External markers and internal landmarks are used to identify corresponding slices on CT and SPECT. Selected CT/SPECT pairs are aligned in the X-Y plane, if necessary, corrected for skew and rotation, and displayed side-by-side using color scales individually optimized for each modality. Simultaneous ROI's are drawn on both images and region statistics are calculated.

"Fusion" of SPECT/CT images helps identify normal "hot" structures on SPECT, localize abnormal activity to specific soft tissue structures on CT, and clarify soft tissue densities on CT as unequivocal tumor. We expect this to be useful in accurate ROI delineation for quantitative analysis.

Posterboard 1219

SIMPLE, ACCURATE, AND REPRODUCIBLE RESOLUTION MEASUREMENTS USING POINT OR LINE SOURCES. J.L. Lancaster and M.F. Hartshorne, UT Health Science Center and Brooke Army Medical Center, San Antonio, TX.

The most commonly accepted index for spatial resolution is the full width at half maximum (FWHM) of the line spread function. The actual implementation of this measurement is often very time consuming and sometimes not as accurate or reproducible as would be desired. The analytical method which we employ is based on the determination of an equivalent width of the line or point spread function. On the assumption that most spread functions are Gaussian like, a known ratio is used to calculate the equivalent FWHM from the equivalent width. Even when the spread functions are not Guassian (i.e. with long tails as with SPECT) the method can be shown to provide good results.

The accuracy and precision of the equivalent FWHM method comes from the fact that the area under of the square of the normalized spread function is used rather than a few selected points. Squaring a Guassian function yields another Gaussian which is reduced in width by 0.707. Squaring the spread function data provides two advantages (1) more significance applied to data near the center of the spread function and (2) a data point at 10% of the peak value for raw data corresponds to a data point of only 1% of the peak value in the squared data. Using data points within the 10% range yields an error in area calculation of less than 0.2% for the squared spread function. This small area error justifies normalization of the spread function within this range.

The method is easily automated on nuclear medicine computer systems and can also be easily calculated off-line using line or point source profile data.

Posterboard 1220

INTERACTIVE RECONSTRUCTION IN SINGLE-PHOTON TOMOGRAPHY. T.R. Miller, J.W. Wallis, and A.D. Wilson. Washington University, St. Louis, MO.

An important consideration in the reconstruction of images in single photon tomography is the choice of filter employed in the filtered backprojection algorithm. A new method was developed to allow interactive selection of the reconstruction filter at the time of image interpretation.

Two changes in the reconstruction process have been made to permit interactive filtering: 1) In the filtered backprojection algorithm, the only part of the reconstruction process requiring user interaction is the selection of the window function. Since the ramp and window filters have different purposes, we have separated them, placing the window at the end of the reconstruction process as a three-dimensional filter (simultaneously obtaining the additional advantages of Z-axis filtering). Thus, all stages of reconstruction except the window function are performed before the physician begins to interpret the study. 2) A three dimensional version of the Chebyshev recursion algorithm was developed to permit

rapid convolution filtering, substantially speeding up the application of the window function.

Using these methods, on a MicroVax II computer without an array processor, single slices from a 64x64x64 data set can be filtered for display in under 1/2 second. When an array processor is employed, it is estimated that the entire cube can be filtered in approximately one second. Thus, the user can interactively choose any desired filter for a given tomographic study at the time of interpretation of the images.

Posterboard 1221

Classification of Thallium-201 Scintigrams Using a Neural Network Trained by Back Propagation.

H. Sochor, G. Dorffner, G. Porenta, University of Vienna Medical School, Vienna, Austria.

The development of computer assisted methods to help with the interpretation of Thallium-201 scintigrams has faced difficulties often associated with pattern recognition tasks. Rule based expert systems commonly used to represent medical knowledge (MYCIN, INTERNIST-1, etc.) most often rely on symbolic data manipulation and therefore are not particularly suited for image processing and interpretation. The parallel distributed processing approach using neural networks trained by appropriate learning schemes provides for a simple method of knowledge acquisition from examples. In a simple pilot project assessing the feasibility of this strategy we used data of 15 scan segments to develop a system discerning between normal patterns and patterns of coronary artery disease. The prototype was implemented on a SYMBOLICS 3600 using VIE-NET, a software tool written in LISP for rapid prototyping of neural network architectures. The neural network consists of 45 clusters of input units with data from 15 segments, an hidden layer with 30 units, and a single output unit. Training is achieved by a back propagation strategy. A pilot study involving 29 scans (12 judged normal by a human expert, 17 with significant 1 or 2 vessel disease) delivered correct classification in all cases.

Dosemetry/Radiobiology

Posterboard 1222

RADIATION MONITORING IN A CLINICAL PET FACILITY: PRELIMINARY EXPOSURE DATA. C. Plott, J. Kam, G. Hathaway, and K. Hubner. Department of Radiology, The University of Tennessee Medical Center at Knoxville, Knoxville, TN.

From the beginning of the PET program at UTMCK, special attention has been given to potential radiation exposure of personnel. A comprehensive, on-going evaluation of monitoring and safety has evolved. Using appropriate devices and instrumentation, total exposure and exposure rates have been documented for all "routine" aspects of clinical PET. Staff activities addressed in our survey include cyclotron operation, radiopharmaceutical production and quality control, performing transmission scans, administering doses to patients, and attending patients during emission scanning.

Current staff includes a radiochemist, pharmacist, medical physicist, and two nuclear medicine technologists. Monitoring of the facility shows that the radiation hazard associated with radiotracer production is not a direct result of the cyclotron operation but rather of the radioactive material produced. Personnel monitoring records indicate that whole body doses are comparable to any other department in radiology. Hand doses, however, are higher than in conventional nuclear medicine and are dependent upon the number of patient studies performed. Nonetheless, with adequate facility design, proper equipment, personnel training, and precautions, radiation exposures are minimized and do not interfere with the progress of a clinical PET facility with high patient through-put. Our facility will be described and detailed data of personnel and environmental monitoring will be presented. Suggestions will be made as to reduce exposure by improving procedures and shielding.

Posterboard 1223

COMPUTATIONAL METHODS FOR ESTIMATION OF ABSORBED DOSE TO TISSUES OF THE BODY FROM THERAPEUTIC APPLICATION OF RADIOLABELED ANTIBODIES. J.C. Ryman, K.F. Eckerman, and M. Cristy. Oak Ridge National Laboratory, Oak Ridge, TN.

We have developed computer codes to estimate the dose to normal tissues from activity distributed in tumor sites within the body. These are extensions to codes which have been used to compute specific absorbed fraction data in target tissues for photon emissions uniformly distributed within source tissues (ORNL/TM-8381/V1, April 1987). The extensions permit the user to define a tumor mass within reference anatomical models for both pediatric and adult patients. Tumors are modeled as the intersection of a sphere with a user-specified organ. Energy deposition within normal tissues is evaluated using Monte Carlo methods to simulate radiation transport or to integrate a point isotropic dose distribution function. We continue to find the latter method an attractive alternative to the more time-consuming simulation of radiation transport. These codes allow the estimation of radiation dose to body tissues from therapeutic applications of radiolabeled antibodies, given the energies and intensities of the emitted radiations and the time course of the administered activity in the body.

Work supported by contract DE-AC05-84-OR21400 between the USDOE and Martin Marietta Energy Systems, Inc.

Posterboard 1224

COMPARISON OF THE CYTOGENETIC EFFECTS OF AUGER ELECTRON- AND ALPHA-EMITTING RADIOISOTOPES. J.L. Schwartz, R. Atcher, P.V. Harper, A. Hughes, J. Rotmensch, S.J. Gatley and E.R. DeSombre. University of Chicago and Argonne National Laboratory.

Both Auger electron and alpha-emitting radioisotopes have been proposed as ligands for receptor-directed radiotherapy. We compared the clastogenic effects of Br-80m, an Auger electron-emitting radionuclide with a 4.4 hr half-life, with Bi-212, an alpha-emitter with a 1 hr half-life, in Chinese hamster ovary (CHO) cells. Because of its short path length, Br-80m was radiotoxic only when incorporated into DNA such as in the form of [Br-80m]BrdUrd. Cells exposed to [Br-80m]BrdUrd for 2 hr in mid-S phase had large numbers of mostly chromatid-type breaks. There was a linear increase of 1 break/cell/μCi exposure as the dose increased from 0 to 6.7 μCi/ml. Many of the cells had multiple aberrations and in some, parts of the chromosomes were shattered and could not be scored accurately. In contrast, a 2 hr exposure of CHO cells to Bi-212 chelated to DTPA, a form which does not enter the cell, induced a linear increase of only 0.2 breaks/cell/μCi exposure. There was no evidence of heavily damaged or shattered chromosomes in the Bi-212 treated cells. Thus Auger-electrons appear to be more clastogenic than the alphas. However, unlike Auger-electrons, alphas need not be in close proximity to the DNA to have clastogenic and therefore radiotoxic effects.

Endocrine

Posterboard 1225

EVALUATION OF THALLIUM-201 WHOLE-BODY SCINTIGRAPHY IN THE DIAGNOSIS OF METASTATIC THYROID CARCINOMA. FL Datz, AJ Scuderi, JE Handy, KA Morton, AJ Fortner. University of Utah School of Medicine, Salt Lake City, Utah.

There is controversy concerning the utility of Tl-201 whole body scintigraphy in the evaluation of metastatic thyroid carcinoma. The purpose of the study was to determine the relative efficacy of Tl-201 scintigraphy in comparison to standard I-131 whole-body scans and serum thyroglobulin levels.

Twenty-three patients with papillary-follicular thyroid carcinoma were studied. Tl-201 whole-body scintigraphy was performed after injecting 2 mCi of Tl-201 intravenously, and imaging with a LFOV camera 20 minutes later. I-131 scans were performed on patients when their TSH was greater than 50 uIU/ml. Ten millicuries of I-131 were given orally, and 72 hours later whole-body imaging was performed. Serum thyroglobulin levels were obtained while the patients were off Synthroid.

For Tl-201 whole-body imaging, the results were: sensitivity .50, specificity .86, positive predictive value .89, negative predictive value .43. For I-131 whole body imaging: sensitivity .93, specificity 1.00, positive predictive value 1.00, negative predictive value .88. In only one case was the Tl-201 positive when the I-131 whole-body scan was negative in a patient with elevated thyroglobulin. In all cases, the degree of Tl-201 uptake was significantly less than I-131 uptake.

We conclude Tl-201 imaging is insufficiently sensitive to replace I-131 whole-body imaging in detection of metastatic disease. Thallium-201 is of little use as an adjunct to I-131 whole-body imaging and thyroglobulin determinations.

Posterboard 1226

FRACTIONATED RADIOIODIDE DOSES COMPARED TO USUAL, SINGLE DOSES FOR ABLATION IN THYROID CANCER. Y. Lee, K. Flannery, H.T. Pretorius, G.A. Wilson, and R.E. O'Mara. University of Rochester Medical Center, Rochester, NY.

We treated 60 thyroid cancer patients with I-131 from 1976 to 1985. The first therapy dose averaged 120 mCi in 45 patients and in the 15 others, two or three fractions of 25 to 50 mCi were given at about weekly intervals for an average initial, total dose of 88 mCi. The two groups were comparable in tumor type, pure follicular carcinoma being 13% of the split dose and 22% of the single dose cases, with all by diagnostic 5 mCi I-131 scans in every case, with average follow-up of 33 months for split dose and 42 months for single dose therapy. Residual neck uptake and retreatment occurred in an identical fraction, 47%, of both groups; another identical fraction of 43% (9/21 single and 3/7 split dose) patients needing retreatment had an initial, total dose less than 70 mCi. To clarify the dose response, 5/15 of split dose patients had less than 70 mCi with 3/5 unsuccessful, while 10/45 (22%) of the single doses were less than 70 mCi, but 90% of these 10 were unsuccessful. Although all patients (n=4) with metastases had single doses and were not completely ablated, the fraction of each group with eventual complete ablation, 14/15 (93%) of split dose and 37/45 (82%) of single dose cases, was similar. In conclusion, with appropriate patient selection, fractionated I-131 therapy can achieve results similar to usual, single dose therapy, provided large, single doses are used for necessary retreatments.

Posterboard 1227

FREQUENT ASSOCIATION OF HOT THYROID NODULE(S) AND PARATHYROID ADENOMA. DIAGNOSIS WITH THALLIUM-TECHNETIUM SCINTIGRAPHY. *J.N. Talbot, **C. Gibold, **M.J. Delisle, *G. Milhaud. *Hôpital Saint-Antoine, Paris, **Institut Jean Godinot, Reims, France.

In 1985, we reported the simultaneous occurence of an autonomous thyroid nodule and a parathyroid adenoma. The former was unexpected and diagnosed during Tl-Tc scintigraphy performed to localize the parathyroid adenoma. We assumed that this association was not casual and performed, during the last two years, Tl-Tc scintigraphy in 147 patients suffering from primary hyperparathyroidism.

A thyroid nodule was palpable in 19 of them. Technetium scintigraphy evidenced a hot nodule in 9 cases (in 3 of them, another hot nodule was discovered) and a cold nodule in 10 cases. The proportion of hot thyroid nodule(s) was 47% in patients suffering from both primary hyperparathyroidism and a solitary palpable nodule of the thyroid.

In comparison, 477 patients referred for a solitary palpable nodule without any evidence of parathyroid gland hyperfunction were submitted to 99m Tc thyroid scintigraphy during the same period of time. The nodule was hot in 42 cases (9%) and cold in 435 cases (91%).

The difference between the frequency of hot nodule(s) in uninodular (or binodular) goitre according to the presence or the absence of a parathyroid adenoma is highly significant (Chi-square with Yates' corredtion: $p<<0.0001$)

We conclude that hot thyroid nodule and parathyroid adenoma are related. Once primary hyperparathyroidism is biologically assessed, Tl-Tc scintigraphy should be performed as it allows the detection of an unexpected hot thyroid nodule as well as the localization of the adenoma. When a hot thyroid nodule is discovered, blood calcium, phosphate and parathyroid hormone levels should be assayed in order to detect silent hyperparathyroidism.

Immunology/Infectious Disease

Posterboard 1228

COMPARISON OF UNLABELED IN-111 CHLORIDE, IN-111 OXINE-LABELED LEUKOCYTES AND IN-111 TROPOLONE-LABELED LEUKOCYTES IN AN EXPERIMENTAL ABSCESS MODEL. N Rofsky, F Datz, A Scuderi, W Bilotta, K Morton, J Handy, P Christian, C Krebs. University of Utah School of Medicine, Salt Lake City, Utah.

There is considerable controversy whether unlabeled In-111 chloride, In-111 oxine-labeled leukocytes, or In-111 tropolone-labeled leukocytes are best for detecting infection. The purpose of this study was to compare these agents in an experimental abscess model.

One hundred forty-four subcutaneous abscesses were created in 18 mongrel dogs using subcutaneously-implanted polyvinyl sponges treated with a standard innoculum of S. aureus from an identical strain. Twenty-four hours after implantation, 6 dogs were injected with In-111 chloride, 6 with In-111 oxine-labeled leukocytes, and 6 with In-111 tropolone-labeled leukocytes. Twenty-four and 48 hours after injection, 3 sponges and their adjacent infected tissues per dog were excised, weighed and assayed for activity. The average values of 3 samples per dog were calculated both at 24 and 48 hours, and expressed as the fraction of the injected dose/gm of excised sponge or tissue.

The relative sponge activity (injected dose/gm) of chloride: oxine: tropolone at 24 hr was 1.0: 19.0: 27.3; and at 48 hr was 1.0: 9.1: 5.1. Relative adjacent infected tissue activity of chloride: oxine: tropolone at 24 hr was 1.0: 6.8: 1.3, and at 48 hr 1.0: 7.1: 1.1, respectively.

Our data indicate labeled leukocytes (oxine and tropolone) localize at much higher concentrations than In-111 chloride in experimental abscesses. Tropolone had higher sponge activity but lower surrounding infected tissue activity at 24 hr compared to oxine.

Instrumentation

Posterboard 1229

COMPARATIVE ANALYSIS OF XE-133 AND XE-127 AS ISOTOPES FOR DYNAMIC SPECT STUDIES OF CEREBRAL BLOOD FLOW (CBF).
D.W. Jones, K.F. Berman, R. Coppola, D.R. Weinberger.
National Institute of Mental Health, Washington, DC.

Although Xe-133 has been used for several years as an isotope for dynamic SPECT studies of cerebral blood flow (CBF), the use of Xe-127 for this purpose has never been systemically explored. The rather scant lore on Xe-127 has ranged from predictions that its 5:1 advantage over Xe-133 in terms of usable counts per unit subject dose and the lower attenuation of its 200 keV imaging gamma would make it an excellent isotope for dynamic SPECT, to suggestions that its higher energy imaging gamma and its 375 keV emissions might make it useless for imaging studies. To address this issue we conducted a comprehensive series of phantom studies comparing the imaging qualities of these two radioxenons and their relative merits in terms of resolution, attenuation, and usable counts per specific activity. Studies were performed on a Medimatic Tomomatic 564 dynamic SPECT scanner using three different collimators with nominal resolutions of 16 mm, 12 mm, and 9 mm. Varying numbers of total counts per image were employed to assess the clinical applicability of all combinations of isotope and collimator.

Our results indicate that Xe-127 is an excellent isotope for dynamic SPECT, generating phantom images far superior to those obtainable with Xe-133, and exhibiting much higher overall sensitivity [cps/(μCi/ml)/slice]:

Collimator:	16 mm	12 mm	9 mm
Xe-127	37 000	24 000	5 700
Xe-133	8 600	4 900	1 800

Use of Xe-127 can improve resolution more than 30% and reduce subject dose twofold. Xe-127 appears to be the radioxenon of choice for clinical SPECT studies of CBF.

Posterboard 1230

HIGH RESOLUTION FOCAL TRANSMISSION IMAGING. S.G. Mirell, R.P. DeVito, J.D. Treffert, M.A. Winston, W.H. Blahd.
VAMC West Los Angeles and UCLA, Los Angeles, CA, and Siemens Gammasonics, Inc., Des Plaines, IL.

Anatomical structure is directly correlated to radiopharmaceutical distribution using a gamma camera densitometer accessory to acquire paired transmission and emission images. The densitometer hardware is comprised of two external sources (60 KeV 200 mCi Am-241 and 122 KeV 50 mCi Co-57) mounted with the gamma ray beams sequentially exposed at the 60 cm focal point of a specially designed low energy converging hole collimator. In the present application, high resolution transmission images are generated in 3 min using only the 60 KeV beam. This mode of transmission imaging is a radical improvement over the planar source with parallel hole collimation techniques previously reported in the literature. The focal geometry of the densitometer configuration inherently combines high spatial (0.5 cm FWHM at 15 cm) and very efficient use of the source flux. The latter typically results in a count rate of 20K/sec for patient studies thereby permitting instantaneous P-scope visualization of structure and facilitating transmission imaging even in the presence of substantial in vivo radiopharmaceutical. The camera system can be switched into the transmission mode whenever a "snapshot" anatomical reference image is required.

Preliminary applications in the lungs and the skeleton have been examined in a series of clinical studies since these two subject areas demonstrate the highest contrast in conventional radiographs. The studies suggest that focal transmission imaging can be a highly effective and easily implemented adjunct to emission imaging.

Posterboard 1231

IMPROVED IMAGE CONTRAST BY SCATTER SUPPRESSION WITH ENERGY WEIGHTED ACQUISITION. P.H. Murphy, S.E. Long, W.H. Moore, R.D. Dhekne, M.J. Blust, B.K. Pounds. St. Luke's Episcopal Hospital, Baylor College of Medicine, Houston, TX.

Relatively poor energy resolution of NaI detectors in scintillation cameras requires acceptance of substantial Compton scattered gamma rays to maintain a reasonable sensitivity. By weighing the contribution of each detected event over most of the energy spectrum instead of in a selective energy window around the photopeak, sensitivity can be maintained while appropriately deemphasizing scattered events and emphasizing those events most likely to be primary, resulting in improved contrast.

Quantitative improvements in target to background ratios were documented in Tc-99m, Tl-201 and Ga-67 images in phantoms and patients by comparing photopeak windowed acquisition to energy weighted acquisitions with an add-on weighted acquisition module (WAM) on a modern gamma camera. Calculated functional parameters, such as ejection fraction, GFR, and polar thallium maps were compared between the two simultaneous acquisition methods. Qualitative improvement was observed in over 60 patient studies with the most significant changes noted in the Ga-67 and Tl-201 images. An increase in focal irregularities of the distribution of Ga-67 was observed in the thorax and abdomen which was not observed in phantoms either with or without scattering media suggesting that the irregularities are real and not an artifact produced by the weighted acquisition. Optimization of the weighting kernel for radionuclide and body region is under continuing development.

Posterboard 1232

PARADOXICAL EFFECT OF THE SKULL ON ATTENUATION CORRECTION REQUIREMENTS FOR BRAIN SPECT. R.L. Nicholson, M. Doherty, K. Wilkins, F.S. Prato. St. Joseph's Health Centre and Univ. of Western Ontario, London, Canada.

A human skull (18x12 cm) filled with $^{99m}Tc\ O_4^-$ in gelatin was imaged by SPECT. Bottle phantoms (15 cm dia) were also imaged with and without a peripheral layer of aluminum foil having electron density, total attenuation and thickness similar to skull. Linear attenuation coefficients (.04-.12 cm^{-1}) were applied and counts/pixel for central vs peripheral ROI's determined. A ratio of 1 indicated best attenuation correction.

The peripheral attenuation of skull or foil unexpectedly reduced the required attenuation correction. Peripheral attenuation reduced edge counts with respect to centre counts in the projection data; a longer ray path for edge counts than central counts through the curved peripheral attenuator apparently reduces edge counts through a combination of attenuation and scatter.

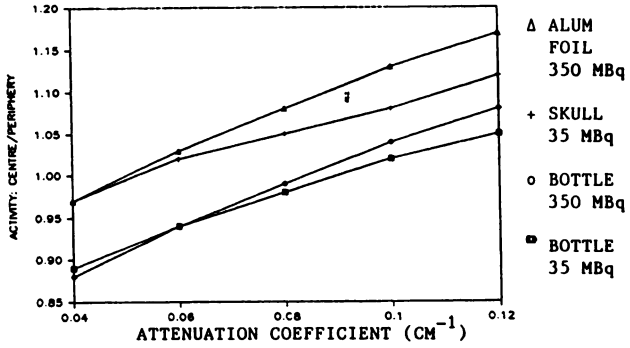

Posterboard 1233

PRECISION AND DOSE LIMITS FOR DPA OF THE SPINE
J.A. Sorenson, B.D. Collick, S.W. Smith, A.P. Hornblad
LUNAR Radiation, Inc., Madison, WI

Precision is critical in DPA (dual-photon absorptiometry) because it limits the detectability of small changes in bone mineral density (BMD). Clinical precision for measurement of spinal BMD has been variously reported as 1.5-4%. We investigated factors that contribute to precision error to determine the ultimate limits of precision and its relationship to patient dose. Theoretical calculations and experimental measurements on realistic spine phantoms indicate that: i) DPA measurements can be performed at the limits of quantum statistics with either Gd-153 or x-ray based DPA systems, ii) For Gd-153 systems, the quantum statistical limit for measurement of spinal (L2-L4) BMD in average patient soft-tissue thickness (18 cm) is approximately 1%, iii) For x-ray based systems, the precision limit for the same measurement is about 0.5%, and, iv) The dose required to achieve these limits is less than 1 mR in both cases. Theoretical and measured doses with Gd-153 in our studies were less than have been reported in the literature (2-20 mR), possibly because of radioactive contaminants in sources used in earlier measurements. Precision per unit dose is superior with x-rays due to better beam collimation (less dose overlap between scan lines), not more optimal selection of x-ray energies.

We conclude that precision of 0.5-1% is possible in DPA measurements of spinal BMD, with patient entrance doses of less than 1 mR. These limits should be approachable in clinical practice with improved image resolution and edge-finding, and more stable electronics; however, better precision at lower doses is not possible, because of inadequate photon statistics.

Neurology

Posterboard 1234

EVIDENCE FOR AXONAL TRANSPORT OF [C-14]-2-DEOXYGLUCOSE.
Robert F. Ackermann and Michael E. Phelps. Division of Nuclear Medicine and Biophysics; Laboratory of Nuclear Medicine (DOE); ULCA School of Medicine, Los Angeles, CA 90024.

We present evidence that some [C-14]-2-deoxyglucose (2DG) taken up by neurons is translocated to distant anatomically-related sites.

Rats were killed 5-72 hours after injection with 1 uCi of 2DG in 0.2 ul normal saline directly into one of several loci: eyeball, hippocampus, and caudate nucleus. The resulting autoradiograms revealed label at the injection site itself, and also in axonal terminal fields of each injection site. With eyeball injections label was found in the contralateral lateral geniculate body and superior colliculus; with hippocampus injections label was found in the ipsilateral lateral septum; and with caudate injections label was found in the ipsilateral substantia nigra.

Caudate injections also produced labeling of various thalamic nuclei not known to receive direct projections from the caudate nucleus. This implies either retrograde transport from the caudate to projecting thalamic nuclei, or transsynaptic orthograde transport via the globus pallidus or entopeduncular nucleus.

Substituion of labeled O-methyl-glucose for 2DG resulted in non-specific labeling in the vicinity of the injection site, and did not result in terminal-field labeling. Therefore, the translocated molecule is 2DG-6-phosphate or a metabolite (e.g., glycogen).

These results suggest that in addition to the general supply provided by capillary networks, energy substrates can be selectively transported via neuronal circuitry.

Posterboard 1235

QUANTITATIVE SPECT EVALUATION OF CEREBRAL PERFUSION IN SCHIZOPHRENIA.
M.B. Cohen, L.S. Graham, R.R. Lake, J. O'Rear, A.S. Kling, L.J. Fitten, E.J. Metter, L.S. Yamada, G.A. Bronca, M.P. Gan, K.L. Greenwell, and R. Sevrin. VAMC, Sepulveda, CA and UCLA, Los Angeles, CA.

Conflicting reports have appeared regarding the presence of areas of cerebral hypoperfusion in Schizophrenics. A SPECT study with I-123, (p,5n)IMP was performed to study this question. Ten chronically medicated patients with well characterized Schizophrenia (S) and five normal subjects (N) were imaged for 50 minutes with a single-headed SPECT camera and a high resolution collimator beginning 20 minutes after the IV injection of 5 mCi I-123 IMP. Preprocessing using a Metz filter and reconstruction with attenuation correction was performed with a PDP 11/84 computer. Perfusion was quantitated in the cortex and basal ganglia using normalization to the uptake in the cerebellum. Small ROIs were quantitated in known areas of cortex with no overlap into adjacent "lobes" using the mean value for the 5 "hottest" pixels in the area of interest. Perfusion was evaluated in 50 regions on transverse, coronal and selected parasaggital slices of 0.6 cm thickness. Symmetrical perfusion was observed in all regions on all projections for both N and S. There was no significant difference (p greater than 0.5) between N and S in either mean values or the range of values for perfusion in any of the 50 regions. Perfusion ratios in the cortical ribbon to cerebellum varied between 0.8 and 0.9 in both groups. An improved method of quantitative SPECT imaging finds no evidence of cerebral hypoperfusion in chronically medicated schizophrenic patients.

Posterboard 1236

REGIONAL CEREBRAL BLOOD FLOW CHANGES IN PATIENTS WITH PANIC DISORDER.
K. Koster, S.W. Woods, E.O. Smith, I.G. Zubal, J.H. Krystal, D.S. Charney, P.B. Hoffer. Yale University, New Haven, CT.

Yohimbine (YOH) is an alpha-2 adrenergic antagonist, which increases noradrenergic function. Patients with panic disorder (PD) show an increased behavioral, cardiovascular and biochemical response to intravenous administration of YOH compared to normals. To assess the possible effect of YOH on regional brain function, we studied regional cerebral blood flow (rCBF) in 4 patients (pts) meeting DSM-III criteria for PD and 3 healthy volunteers (HV). Each subject was studied in random sequence on separate days after intravenous infusion of YOH (0.4 mg/kg) or placebo infusion (saline). At the height of the behavioral effect, directly following the infusion of drug or placebo 740MBq of Tc-99m HMPAO was injected intravenously under standardized conditions. Transaxial images of the brain were obtained 1 hour later with a multicrystal SPECT gamma camera (Strichman 810X). Ratios of selected region of interest (ROI) to cerebellum and asymmetry indices were calculated. All patients experienced higher anxiety levels and robust changes in frontal cortex bilaterally (-10.8 ± 9.7 % on left, and -11.2 ± 7.7% on the right) as well as unilateral changes in thalamic bloodflow with YOH. The unilateral changes correlated with hand preference. The HV showed none of the behavioral or rCBF changes.

We conclude that 1) SPECT rCBF studies are feasible in patients with PD after pharmacologic induction of anxiety, 2) YOH alters rCBF in pts with PD and 3) noradrenergic disregulation of frontal cortical and thalamic perfusion or function may play a role in PD.

Posterboard 1237

KINETIC EVALUATION OF THE OPIATE RECEPTOR LIGAND H3-CYCLOFOXY (CF) IN RAT BRAIN: I.V. INFUSION (0.3-3 min) AND I.V. BOLUS INJECTION (1-60 min) EXPERIMENTS.
Y. Sawada, M. McMannaway, R. Kawai, S. Hiraga, M. Channing and R.G. Blasberg. NIH, Bethesda, MD 20892

A 3 compartment model ["free" CF in brain, nonspecifically bound CF, and CF bound to a high affinity opiate receptor] was used to fit time-activity data of tracer CF in brain and blood that was corrected for metabolites measured by ethylacetate extraction and

HPLC. Vascular transport (PS1, k2), nonspecific binding expressed as an equilibrium constant (Keq), the rate constant for binding to the opiate receptor (k3) and the off rate constant (k4) were estimated. For thalamus (opiate rich) these values were: 2.6 ±1.9 ml/min/g, 4.8 ±7.6/min, 0.8 ±1.3, 4.1 ±0.8/min and 0.14 ±0.03/min, respectively. For cerebellum (opiate poor) the values were 1.6 ±0.4, 3.0 ±3.3, 0.96 ±1.7, 15 ±21 and 4.9 ±7.1. The PS1/k2 ratio was 0.54 ±0.33 and 0.53 ±0.21 ml/g, respectively, and approximates $fb \cdot \lambda$ (0.51 ml/g), the calculated volume of "free" ligand distribution in tissue (where fb = "free fraction" in blood and λ = tissue water patition coefficient). The total vol-ume of distribution of CF in thalamus and cerebellum was 16.1 and 2.5 ml/g. Similar values and good fits of the data were obtained by assuming PS1/k2 = $fb \cdot \lambda$; this analysis suggests a defined relationship between the "free concentration" of ligand measured in blood and the "free concentration" in tissue water, and reduces the number of parameters by one. The binding of CF to blood elements (fb=0.58 and Cb/Cp =1.3) and nonspecfic binding in brain tissue (Keq) is weak; specific binding (the binding potential) to opiate receptors in cerebellum is low (k3/k4 = 3.1 ±2.2) in comparison to that in thalamus (k3/k4 = 28 ±3); and k4 in thalamus is sufficiently high so equilibrium studies can be performed. Thus, it should be possible to clearly visualize and estimate regional concentrations of brain opiate receptors in vivo using CF and PET.

Posterboard 1238

EVALUATION OF CEREBRAL HEMODYNAMICS BY REGIONAL CEREBRAL BLOOD FLOW(rCBF), REGIONAL CEREBRAL BLOOD VOLUME(rCBV) AND rCBV/rCBF WITH SPECT. H. Toyama, G. Takeshita, A. Takeuchi, H. Anno, K. Ejiri, K. Katada, S. Koga, N. Ishiyama*, T. Kanno* and N. Yamaoka**. Departments of Radiology and Neurosurgery*, Fujita Gakuen Health University School of Medicine, Toyoake and Shimadzu Corp. **, Kyoto, Japan.

To evaluate cerebral hemodynamics by rCBF, rCBV and rCBV/rCBF, 9 normal volunteers and 15 patients with chronic occlusion or severe stenosis of the internal carotid or middle cerebral artery but without a massive low density area on X-CT were studied by using a ring-type SPECT "HEADTOME". We obtained rCBF using Xe-133 inhalation and rCBV with in vivo labelled Tc-99m red blood cells (mean labelling rate 97.3%) and calculated rCBV/rCBF on the same axial plane of the coordinate and displayed by each data. In 9 normal volunteers aged 43-70 years (mean 59.8±8.3), mean rCBF was 45.8±5.12 (ml/100 g brain/min), mean rCBV was 3.98±0.39(ml/100 g brain) and mean rCBV/rCBF was 5.2±0.57 (sec). Values of the affected hemispheres of 15 patients(19 lesions)were classified into 4 types compared with mean rCBF and mean rCBV of normal volunteers as follows. Type I (n=5):rCBF, rCBV were normal, type II (n=3):rCBF was normal, but rCBV increased, type III (n=6):rCBF decreased, and rCBV increased, type IV (n=5):rCBF decreased, but rCBV was normal. On 2 cases of type III, extracranial-intracranial arterial (EC/IC) bypass surgery was performed. Postoperative SPECT showed remarkable improvement by increased rCBF and reduced rCBV in the affected hemisphere in both cases. Furthermore, the large value of rCBV/rCBF in the affected hemisphere was decreased postoperatively. PET studies have shown good correlation between rCBV/rCBF and oxygen extraction fraction(OEF). Our findings suggest that the pattern of type III indicates the misery perfusion area and viable tissue. We propose rCBF, rCBV and rCBV/rCBF with SPECT to be good indicators of cerebral circulatory reserve and EC/IC bypass.

Posterboard 1239

RETT SYNDROME: PET METABOLIC-CLINICAL CORRELATES. D.F. Wong, S. Naidu, P. Sanchez Roa, V. Villemagne, M. Yaster, R.F. Dannals, J. Links, A. Wilson, H. Ravert, J. Harris, H.N. Wagner, Jr., H. Moser. Johns Hopkins Med. Inst. & Kennedy Institute, Baltimore, MD.

Rett syndrome is a disorder affecting females from early childhood with microcephaly, seizures, and stereotypic handwringing behavior. The etiology of this disorder is uncertain and pathological studies have been non-specific. One qualitative study with C-11 NMSP evaluating D2 dopamine receptors in the caudate and putamen in this disorder has been reported. In the present study glucose metabolism was measured with FDG PET in 3 subjects aged 4, 6 and 13 years. In 2 sedated subjects relative metabolic rates showed heterogenous decreases in some areas compared to previously published, awake age and sex matched controls. There was an increase in anterior-posterior and laterality ratios, with markedly lower metabolism in occipital (non visual) and normal to slightly decreased metabolism in parietal and temporal lobes (assuming no regional effects of sedation). There was a slight increase in activity over the frontal regions, and increase in left/right ratio with relative sparing of the sensory motor cortex.

The correlation of EEG abnormalities with areas of hypometabolism in the temporal, posterior parietal and occipital regions is of interest and might explain the degree of dementia resulting from involvement of vital association areas in this disorder. These metabolic patterns were somewhat different from those previously reported in Down's Syndrome and Alzheimer's disease.

Nuclear Magnetic Resonance

Posterboard 1240

SPIN ECHO MAGNETIC RESONANCE IMAGING IN ASSESSMENT OF LEFT VENTRICULAR FUNCTION. M. Ahmad, and R.F. Johnson, Jr. The University of Texas Medical Branch at Galveston, Galveston, Tx.

To test the ability of spin echo magnetic resonance imaging (MR) in obtaining quantitative left ventricular function data, we obtained ECG gated short axis images of the left ventricle (LV) in 13 patients in a 0.6 Tesla Technicare magnet. Multislice imaging sequence was used and five 1 cm thick parallel slices obtained from the base to the apex of the LV during the systolic phase of the cardiac cycle (first 400 msec following the ECG R-wave). The data included 50 images representing 5 slices and 2 echos per slice with each slice recorded five times during the 400 msec imaging interval. Left ventricular endocardium was demarcated and the area of the left ventricular chamber planimetered in the starting image (diastole) and the last image (systole) of each slice. The percentage change in left ventricular chamber area (LVA%) was calculated by subtracting the systolic from the diastolic chamber area and multiplied by 100. LVA% obtained by MR correlated well with LVA% obtained from cine loop of 2-D echocardiographic images of comparable LV short axis slices acquired during 400 msec following the ECG R-wave (r=0.96). Ten patients without complications over a 2-year followup period had a normal LVA% (>30). Three patients with complications (congestive cardiac failure in 2 patients and death in 1 patient) had LVA% of <17.

These data indicate that spin echo magnetic resonance images can be acquired and analyzed in a manner that may provide quantitative information comparable to cine mode images obtained by echocardiography.

Posterboard 1241

CLEARANCE, ORGAN DISTRIBUTION, AND MRI OF CARBOXYLIC ACID DERIVATIVES OF DESFERRIOXAMINE B: K. A. Muetterties, D. L. White, J. M. Tongol, B. L Engelstad, M. G. Wikström, C. L. Roco, and M. E. Moseley, UCSF, San Francisco, CA.

The Fe(III) chelate of the siderophore desferrioxamine B (DF) is an MRI contrast agent that gives both renal and hepatobiliary enhancement. The coordination properties, charge, and lipophilicity of DF can be changed by modification of its structure. The aim of this study was to prepare a number of carboxylic acid derivatives of DF, determine the clearance rates and organ distributions of radiolabeled analogues, and investigate their MRI behavior.

N-succinyldesferrioxamine B (SDF), N-glutaryl-desferrioxamine B (GDF), and N-(3-phenylglutaryl)-desferrioxamine B, were synthesized from the corresponding anhydrides and DF. Complexation of each ligand with $^{59}FeCl_3$ gave a single radiolabeled agent. For the ^{59}Fe studies, groups of four male S/D rats were anesthetized and injected i.v. with radiolabeled agent at pharmacological level (10^{-1} mmole/kg, 1-2uCi/dose). The rats were immediately counted in a chamber gamma counter, and then placed in metabolic cages. Each animal and its excreta were counted at selected time

points up to 7 days, sacrificed on day 7, and dissected. Coronal MR T1-weighted imaging was performed (TR=380 ms, TE=15 ms, 3 mm slices) on a GE CSI-2T unit.

The 7 day organ distributions of all four agents were similar. Fe-DF, Fe-SDF, and Fe-GDF all showed rapid whole body clearance with similar urine and fecal excretion rates. Fe-PGDF also showed similar whole body clearance, but with a *significantly greater fecal and less urinary excretion*. Fe-PGDF produced higher liver and lower kidney MRI enhancement than Fe-DF. In addition, it gave dramatic enhancement in the gut lumen as early as 15 min post injection.

SDF and GDF differ from DF principally in net charge, and the clearance of their Fe chelates was essentially the same as DF. However, the addition of a phenyl group to the chelate backbone produced a dramatic increase in fecal excretion of Fe-PGDF. This may be due to greater lipophilicity of the metal-ligand complex compared to Fe-DF. The MRI renal and hepatic enhancement patterns paralleled the clearance data. The striking Fe-PGDF gut lumen enhancement was consistent with the increased fecal excretion.

Posterboard 1242

PHARMACOKINETIC STUDIES OF IRON-CONTAINING MRI CONTRAST AGENTS. C. L. Roco, J. M. Tongol, D. C. Price, D. L. White, J. P. Huberty, K. A. Muetterties, and B. L. Engelstad, (UCSF, San Francisco, CA); T. Sargent (UC-Berkeley, Berkeley, CA).

This investigation was undertaken to study the in vivo kinetics of iron-containing contrast agents potentially useful for MRI and MRS.

Healthy male adult human subjects were studied after receiving 1-10 uCi of Fe-59- labelled no-carrier-added doses. Selected agents consisted of two stable chelates, Ferrioxamine B (Fe-DF) and Fe-N,N'-bis(o-hydroxy-benzyl)ethylenediaaminediacetic acid (Fe-HBED), and a superparamagnetic iron oxide (AMI-25, Advanced Magnetics, Inc., Cambridge, MA). Subjects were serially counted using a whole body counter for measurement of whole-body retention. Stool and urine samples obtained for 3 days after administration were likewise counted in chamber counting devices. Red cell incorporation was measured using conventional well-counting and Cr-51 red cell mass measurements.

Percent Injected Dose (SD) of Fe-59

	Whole-Body @ Day 14	Urine* @ Day 3	Feces* @ Day 3	RBC @ Day 7
Fe-DF	34 (0.4)	61 (2)	<1%	13 (2)
Fe-HBED	42 (13)	40 (24)	4 (2)[1]	14 (3)
AMI-25	100	0	0	16 (5)

*Cumulative.

Radioiron retention in humans represents iron-loading or isotopic exchange. Exogenous iron in healthy humans is avidly conserved and entered the endogenous iron pool as evident by the long lived plasma component and red cell incorporation of the chelated radioiron. Both Fe-HBED and Fe-DF were excreted principally through the kidneys. AMI-25 was not excreted and, unlike conventional reticuloendothelial agents, is biodegradable in humans as evidenced by incorporation into red cells.

Posterboard 1243

PHASE-ENCODED VELOCITY MEASUREMENTS USING NMR IMAGING. R.E. Wendt III, W.R. Nitz, R. Rokey and P.H. Murphy. Baylor College of Medicine, Houston TX.

Nuclear magnetic resonance imaging may be used to measure velocities *in vivo*. We have developed a velocity-encoding gradient-refocussed echo pulse sequence which is readily implemented on commercial NMR imagers including the use of standard three-dimensional Fourier transform image reconstruction. The resulting data are a set of two-dimensional images in which the intensity of each pixel is proportional to the fraction of spins in that voxel moving with a velocity in the range of that image. The velocities measured are either transverse to the imaging plane or vertical or horizontal within it. A typical data set contains fifteen images with velocity separations of 15 cm/s. A velocity distribution for a region such as the lumen of a vessel is achieved by plotting the mean of the ROI in each image as a function of velocity.

The pulse sequence has been tested both on a phantom and on a normal volunteer. The phantom is constructed of poly-vinyl chloride pipes with inside diameters of 3.8 cm and 1.75 cm and contains a constricted section and a section in which the smaller pipe sends a jet of fluid into the larger. A flow rate of 5.6 l/min produced average velocities of 8.2 cm/s in the larger pipe and 39 cm/s in the smaller pipe. The Reynolds numbers were about 3100 and 6800, respectively. The flow regime was disturbed or turbulent in the entire phantom at this flow rate. The velocity distributions measured by NMR are consistent with "partial plug" flow. The normal volunteer was imaged in the transverse plane in the region of the heart. The acquisition of data was synchronized to the volunteer's ECG and five data sets were collected at 100 ms intervals. A tip angle of 30° was used to reduce the partial saturation of stationary and slowly moving spins. The velocity distributions in the major vessels were also measured by Doppler ultrasound and agree with the NMR velocity measurements.

Posterboard 1244

CLEARANCE, EXCRETION, AND ORGAN DISTRIBUTION OF A NEW MRI CONTRAST AGENT MANGANESE-DIPYRIDOXAL- DIPHOSPHATE (Mn-DPDP). D. L. White, J. M. Tongol, C. L. Roco, K. A. Muetterties, and B. L. Engelstad (UCSF, San Francisco, CA); S. M. Rocklage, W. P. Cacheris, and S. C. Quay (Salutar, Inc. Sunnyvale, CA).

The manganese(II) chelate of N,N'-bis(pyridoxyl-5-phosphate)-ethylenediamine-N,N'-diacetate (DPDP) is a MRI contrast agent useful for liver and heart imaging. This study was undertaken to determine the rate of whole-body clearance, relative renal vs. fecal excretion, and organ distribution of Mn-54 after administration as the DPDP complex at tracer and pharmacologic doses.

Four S/D rats were each anesthetized, injected i.v. with Mn-54-DPDP, immediately counted in a chamber gamma counter, and then placed in a metabolic cage. Each animal and its excreta were counted at selected time points up to 7 d. At Day 7, the animals were sacrificed and dissected, and their organs were counted. An analogous control experiment was performed using Mn-54 chloride.

% Injected Dose (SD) of Mn-54 After 7 Days

	Cumulative Feces	Cumulative Urine	Whole Body	Liver (per g)
Carrier	47 (1)	43 (2)	6 (9)	0.21 (3)
Tracer	45 (5)	22 (3)	37 (3)	1.47 (7)
$MnCl_2$	53 (2)	< 0.3	43 (3)	1.5 (1)

All recovered within the first 6 hrs.

Complexation of Mn by DPDP resulted in significant urinary excretion. A carrier effect was also evident. The fecal excretion could reflect partial dissociation of the Mn from the complex and/or excretion of the intact complex. The mechanism has not yet been determined.

Posterboard 1245

MRI BRAIN VOLUMETRICS FOR AIDS PATIENTS. Nai-Chuen Yang, Peter K. Leichner, Godfrey D. Pearlson, Jose A. Mendizabal, Mary Bascom, and William G. Hawkins. Department of Radiation Oncology and Department of Psychiatry, The Johns Hopkins Hospital, Baltimore, Md.

HIV positive AIDS patients with or without dementia are being studied with brain MRI spin echo transaxial images from a GE machine of magnetic field 1.5 Tesla. Semi-automated computer software is used to contour the brains. The cerebrospinal fluid (CSF) with the brightest signal intensities in spin echo two image is separated out with an eyeball threshold and a masking data set is generated. This information is carried to spin echo one image and a masked histogram with the signal intensity distributions of the white matter and gray matter is generated for each slice.

A global histogram by summing all the slices is then fitted with a two-gaussian model. The intersection point of the two gaussians is used to separate the white matter from the gray matter and their volumes are calculated separately. Compared with persons at risk, preliminary studies of AIDS patients with dementia show the evidence of demyelination, loss of the brain's white matter.

Oncology/Hematology

Posterboard 1246

CORRELATION BETWEEN SERUM PROSTATE SPECIFIC ANTIGEN (PSA) LEVELS AND BONE SCAN FINDINGS IN PATIENTS WITH KNOWN PROSTATIC CARCINOMA. B. Austin, F. Quadri, and M. Blend, Michael Reese Hospital, Chicago, IL and H. Mermall, Hines VAH, Hines, IL.

Prostate specific antigen serum level, a circulating tumor marker for prostate cancer (P.C.), has been proposed as a useful tool in the work-up, staging and monitoring of this disease. The purpose of this study was to correlate serum PSA levels in P.C. patients with and without metastatic bone disease as determined by radionuclide bone scan. Conventional bone scans were performed on 29 patients with known P.C. and on 15 patients with no known cancer history. Blood samples were drawn the day of scanning and PSA levels were determined using an immunoradiometric method. A dual monoclonal antibody sandwich technique with antibodies directed against different antigenic sites on the PSA molecule was used. Bone scans were read without prior knowledge of PSA levels. Of the 29 patients, 3 were excluded because of questionable bone scan results, and 4 were excluded due to recent prostate surgery or manipulation. Using a PSA value of < 4 ng/ml as normal, the following results were obtained: PSA > 4 without mets = 1; PSA > 4 with mets = 8; PSA < 4 without mets = 13; PSA < 4 with mets = 0. Used as a predictor of metastatic bone disease, PSA had a sensitivity of 89%, a specificity of 100% and a negative predictive value of 100%. Based on these values a low PSA may help to exclude metastasis in patients with a questionable bone scan. PSA may also prove useful as a marker for monitoring the course of prostate cancer.

Posterboard 1247

99mTc HMPAO LABELED LEUCOCYTES FOR BONE MARROW SCINTIGRAPHY? COMPARISON TO 99mTc HSA COLLOIDS RESULTS. P. Bourgeois, M. Stegen, G. Demonceau and W. Feremans*.
Dept. of Nuclear Medicine and of Internal Medecine*, C.H.J. Bracops, Free University of Brussels, 79, Rue Dr. Huet, 1070 Brussels, Belgium.

Bone Marrow Scintigrams (BMLSc) have been obtained two to six hours and/or 20 to 24 hours after injection of 8 to 12 millicuries of 99mTc HMPAO labeled polymorphonuclear leucocytes (PMN), in 16 patients (7 males, 9 females, mean age : 53 y.) either with benign or malignant hemopathy, or with benign or metastatic skeletal diseases.

They have been compared within the week thereafter to corresponding pictures (BMCSc) obtained 20 min. after injection of 10 millicuries of 99mTc labeled Human Serum Albumin nanosized colloids.

Except in one case ("false" negative BMCSc - "true" positive BMLSc), 99mTc HMPAO labeled PMN distribution at the level of the bone marrow was exactly the same as of the colloids. However, related to the low activity in the liver with PMN, BMLSc allowed a better delineation and investigation of the lumbar and lowest thoracic vertebras - than did BMCSc - with, in one case, the demonstration of a lesion unsuspected by any other way.

It is concluded that BMLSc may replace BMCSc and be usefull in cases of dubious conventional osseous scintigraphic lesions as well as of neurological or skeletal symptoms involving the lumbar and/or low thoracic regions.

Posterboard 1248

EFFECT OF METHOTREXATE ON THE METABOLIC FATE OF N-13 LABEL FROM L-GLUTAMATE IN A TRANSPLANTABLE RAT TUMOR. S. Filc-DeRicco and A.S. Gelbard. Memorial Sloan-Kettering Cancer Center, New York, NY.

Changes in uptake of label from L-[N-13] glutamate (N-13 Glu) in human tumors after treatment with methotrexate (MTX) have proven useful in determining the response of the tumors to chemotherapy.

To investigate the mechanisms of change in accumulation of label in tumors, we studied the metabolic fate of N-13 Glu in control and MTX treated Walker-256 carcinosarcoma. The tumor was implanted under the renal capsule of female Sprague-Dawley rats. After a period of 7-10 days, the implanted animals were injected, intravenously, with a dose of 30 mg/kg MTX., N-13 Glu was injected into the renal artery 2 hr after treatment and the animals were sacrificed 5 min post injection.. Acid soluble extracts of tumor and kidney (host tissue) were analyzed by HPLC (SCX). In both tissue extracts, more glutamate was metabolized after treatment with MTX. In untreated tumor, the predominant labeled metabolite from N-13 Glu was aspartate (70%), with glutamine (18%), alanine (5%), urea (4%) and ammonia (2%) also present. After treatment with MTX, aspartate accounted for only 17% of the labeled metabolites from N-13 glu, while urea and alanine increased to 19% and 33%, respectively. In kidney extracts, MTX treatment resulted in a decrease in the percent of label in aspartate (from 50% to 24%) and in glutamine (from 25% to 9%). Conversely, the percent of label in ammonia increased from 13% to 49%, and in urea from 9% to 16%.

These studies demonstrate a profound change in the distribution of label from N-13 Glu in tumor and kidney tissues after treatment with MTX.

Posterboard 1249

A MODELING ANALYSIS OF IgG, F(ab')2, AND Fab PERCOLATION THROUGH TUMORS. K.Fujimori, J.N.Weinstein, D.G.Covell, and J.E.Fletcher. National Institutes of Health, Bethesda, MD.

After many clinical trials of monoclonal antibodies (MAb), it is clear that a quantitative understanding of MAb distribution would be helpful for selecting the particular type of MAb or optimizing the dosage.

The percolation of MAb through tumors was simulated on a microscopic scale by considering: 1) Molecular weight and valency of MAb, 2) Pharmacokinetics of MAb following iv injection, 3) MAb permeability through capillary endothelium, 4) MAb diffusion and convection in tissues, 5) Antigen-MAb interactions, 6) MAb metabolism. The partial differential equations describing this model were solved numerically (by a collocation method). Model parameters were based on literature values, clinical studies, animal experiments, and in vitro analysis of MAb binding characteristics. A specificity ratio, an index of spatial uniformity, and the concentration of MAb were calculated as a function of time and position in the "tumor".

In general, higher MAb diffusion coefficients resulted in greater specificity and more uniform distribution throughout the tumor. The average tumor MAb concentration was not linearly related to the MAb dose. In addition, the specificity decreased as the dose increased. As the affinity of Fab increased,both average specificity and concentration increased considerably; a similar increase of affinity for IgG produced much less change in these variables. The average concentration, specificity, and spatial uniformity decreased when the rate of MAb metabolism increased.

These models of MAb percolation through tumor, coupled with results of global MAb pharmacokinetics, can be helpful in the design and analysis of clinical studies.

Posterboard 1250

FACTOR ANALYSIS OF (F-18)DEOXYGLUCOSE DYNAMIC STUDIES IN CANCER PATIENTS. M.Furudate, K.Fujimori, M.Matsuda*. Hokkaido University,Sapporo, *Nikko Memorial Hospital, Muroran, Japan.

Recently, (F-18) deoxyglucose (FDG) has been used as a tumor seeking agent. The theory of (F-18)FDG accumulation in tumor is more understandable than that of Ga-67 citrate, but the sensitivity of tumor diagnosis is not excellent. To enhance the tumor visualization and evaluate the

heterogeneity of tumor, dynamic images were analyzed by the factor analysis in cancer patients.

We performed 16 studies in 15 patients, 10 were lung cancer and 5 were abdominal cancer. After iv administration of 3-5mCi of (F-18)FDG, dynamic images were taken 15 sec/frame x 240 frames by LFOV camera equipped the special high energy collimator for positron and recorded in Scintipac 2400 computer system. Whole body images were taken at 60 minutes after administration. The functional images, the number of factors were 2,3, and 4, were created by the two dimensional factor analysis method and compared to original images.

The image of increasing factor showed the margin and location of tumors clearly in 10 studies. 3 studies were not significantly different from original images. Tumors were not visualized in 3 studies on either original images or functional images. Tumors were visualized unhomogeneously as the number of factors were increased. It could be estimated a heterogeneity in tumors. The images of the decreasing factors showed lung and liver. One metastasis, clinically silent, of left adrenal gland was found by the whole body image.

The factor analysis of the dynamic images shows the margin of the tumor clearly and contributes the sensitivity of tumor diagnosis.

Posterboard 1251

IMAGING OF SOFT TISSUE SARCOMAS WITH In-111-LABELED MONOCLONAL ANTIMYOSIN ANTIBODY FRAGMENTS. K. Kairemo, T. Wiklund, K. Liewendahl, J. Heikkonen, M. Miettinen, H. Aronen, A-L. Brownell, and C. Blomqvist. Div. of Nuclear Medicine and Dept. of Radiotherapy and Oncology, Helsinki University Hospital, Finland.

Leiomyosarcoma and rhabdomyosarcoma cells are known to contain myosin. As cell membrane damage occurs in active disease an antibody raised against myosin could be useful for imaging of myosarcomas. In this study we have compared the uptake of radiolabeled antimyosin antibody in various soft tissue sarcomas.

11 patients with soft tissue sarcoma (3 leiomyosarcomas, 3 rhabdomyosarcomas, 2 Ewing sarcomas, 1 synovial cell sarcoma, 1 neurofibrosarcoma, 1 maldifferentiated sarcoma) were studied at least twice after intravenous injection of monoclonal antimyosin R11D10-antibody Fab-fragments (DTPA-derivative with In-111-label). Whole body scintigraphy was performed in all cases. Various subtraction methods using Tc-99m-tracers (tin colloid for liver-spleen; DTPA for kidneys; MAA for lungs) were employed in order to improve interpretation of images. In one case a brain SPECT study was performed.

Of a total of 60 previously known lesions (CT, US, MRI) 54 were detected by immunoscintigraphy. The 6 undetectable lesions were in the patients with synovial cell sarcoma and neurofibrosarcoma suggesting that these tumors do not contain myosin. In immunoscintigraphy a total of 66 lesions were identified showing that 12 metastases not known in advance could be localized by this method. These 12 lesions were subsequently verified by other diagnostic methods. We conclude that radiolabeled antimyosin antibody is very useful for staging of myosarcomas.

Posterboard 1252

Evaluation of diagnostic accuracy of Indium-111-labeled murine monoclonal antibody in patients with metastatic breast cancer. S.I.Kim, D.C.P.Chen, E.Yeo, J.Leong, M.E.Siegel, F.Muggia, Division of Nuclear Medicine and Oncology, LAC/USC Medical Center, Los Angeles, CA. 90033

Radionuclide labeled monoclonal antibody (MoAB) imaging to various types of cancer has been tested to detect metastatic lesions with variable success. We evaluated diagnostic accuracy of Indium-111-labeled murine monoclonal antibody in patients with metastatic breast cancer.

Ten patients with known metastatic lesions underwent scans following intravenous injection of 2 mCi of Indium-111 labeled 10-3D2 F(ab')2 MoAB (1mg). Whole body was scanned on a gamma camera 24, and 48 hours after injection. Each patient has single or multiple metastatic lesions in one or multiple organ sites. The results of MoAB imaging were compared to other imaging techniques, such as, CT scan, X-ray, or bone scan.

All metastatic lesions in lymphnodes(2 patients), liver(1), lung(1), and brain(1) showed increased uptake. Out of 2 patients with subcutaneous metastatic lesions, 1 patient had positive scan. However, only 2 patients among 7 patients with metastatic bone disease showed increased uptake. None of bone lesions in spine, rib and pelvis was detected. About 50 % of lesions in skull, sternum and femur were positive. No adverse reaction was noted except one patient who developed skin rash 1 week later.

Our preliminary data showed that anti-breast MoAB imaging can detect metastatic lesions in lymphnodes, liver, lung, skin, and brain. However, metastatic bone lesions were not detected in most of patients.

Posterboard 1253

DEVELOPMENT OF A POTENTIAL DIAGNOSTIC AGENT FOR PROSTATIC CARCINOMA: 4-[*I]-IODOTESTOSTERONE-6-ENE. I. Koslowsky#, L.I. Wiebe#, A.J. McEwan+, J.R. Scott+, V. Somayaji#, R. Hooper+, and R. Flanagan++. University of Alberta# and Cross Cancer Institute+, Edmonton, AB, Canada; Merck Frosst Canada Inc., Pointe Claire-Dorval, PQ++.

The aim of this project is to develop a radioiodinated testosterone derivative which will localize in androgen-receptor positive tumours of prostatic origin.

Radiolabeling of 4-chloromercuritestosterone-6-ene resulted in 4-[I-131]-iodotestosterone-6-ene which was purified by HPLC. Tissue distribution studies were carried out using male mice. Accumulation of radioactivity in the prostate gland and seminal vesicles increased with time, reaching a maximum of approximately 10% of the injected dose per gram of prostate gland at 4 hours, and 12% per gram of seminal vesicles 60 minutes post-injection.

The radiation dose to the whole body and major organs was calculated for I-123. The critical organs were the stomach and intestinal tract (11 mGy/100 MBq); whole body dose was calculated to be 1.1 mGy/100 MBq.

These results indicate that this product may be of value for imaging prostatic carcinoma. Evaluation of this compound in rats implanted with Dunning R3327H tumours has been started.

Posterboard 1254

NUCLEAR MAGNETIC RESONANCE IMAGING (NMRI) OF LIPOSARCOMA J. London, E.E. Kim, A. Shirkhoda, J. Coan, S. Wallace, University of Texas System Cancer Center, Houston, TX

Liposarcoma is the most common malignant tumor in the retroperitoneum and occurs with increasing frequency in advanced age. Survival rate depends on histologic types.

Patients with histologic diagnosis of liposarcoma are prospectively examined to evaluate the NMRI findings related to different histologic types of the tumor and also compare the diagnostic sensitivity of NMRI and CT scans.

There were five different subgroups of proven liposarcoma (myxoid, pleomorphic, atypical lipomatous tumor, dedifferentiated and unclassified) in 9 males and 6 females with age ranging from 25 to 78 years. NMRI was performed using 1.5T imaging system (General Electric Co.) and spin-echo technique in 9 patients and CT with

and without contrast injection was obtained using GE 9800 scanner in 7 patients.

Eight patients had their primary tumors in the abdomen including pelvis, and the other seven lesions were located in the lower extremity. Six abdominal tumors metastatasized or recurred locally, and two of them could not be detected by the CT scan. There was no specific NMRI appearance for any subgroup of liposarcoma. Their heterogeneous signal intensity ranged from low to high on T1- or T2-weighted pulse sequence images.

In conclusion, NMRI displaying excellent soft tissue detail proves to be more accurate than CT for evaluation of liposarcomas, can precisely outline the borders of tumors, evaluate adjacent bone or soft tissue invasion, or involvement of the vascular or lymph nodes. NMRI should be a primary modality for evaluation of the tumor particularly in the abdomen where it can mimic bowel loops.

Posterboard 1255

COMPARISON OF In-111 MONOCLONAL ANTIBODY, Ga-67 CITRATE AND I-123 IMP FOR THE DETECTION OF MALIGNANT MELANOMA.

S. Minoshima, K. Uno, K. Yoshikawa, K. Imazeki, K. Murakami, N. Arimizu, M. Kobayashi, M. Fujita and S. Okamoto. Chiba University School of Medicine, Chiba, Japan.

The detection of malignant melanoma(MM) by radionuclide imaging using with In-111 HTT-97 monoclonal antibody(In-111 MoAb, Hybritech), Ga-67 citrate and I-123 N-isopropyl p-iodoamphetamine(I-123 IMP) was evaluated. Fifteen lesions of recurrent or metastatic MM in 4 patients were proved by clinical evaluation and radiologic examinations, including CT and MRI. 3 mCi of In-111 MoAb was administered to the patients with dripping infusion for 60 minutes and was imaged at 24 hrs, 72 hrs and 120 hrs. Ga-67 citrate was imaged at 72 hrs after 2 mCi intravenous injection. 3 mCi of I-123 IMP was administered intravenously and imaged at 4 hrs. Anterior and posterior spot images were obtained in all patients. These triple examinations were performed within 2-4 weeks 6/15 lesions were detected by In-111 MoAb, 14/15 lesions by Ga-67 citrate and 11/15 lesions by I-123 IMP, respectively.

In conclusion best images of In-111 MoAb were obtained at 72 hrs films. Ga-67 citrate imaging was highest detectability of MM in these three examinations. Images of I-123 IMP were needed later images than ones at 4 hrs, because of its high accumulation of liver and lungs. I-123 IMP appears to be useful agent for the detection of bone metastases in MM.

Posterboard 1256

UPTAKE OF CD-109, A METALLOTHIONEIN-BINDING RADIOMETAL, IN TUMORS IN MICE.

K. Morton, M.D., F. Datz, M.D. and N. Alazraki, M.D., Univ. of Utah, S.L.C., UT 84132 and Emory Univ., Atlanta, GA 30322.

Metallothionein (MT) is an intracellular protein which binds many radiometals having imaging or radiotherapeutic potential. Since MT is increased in rapidly dividing cells in-vitro and during embryogenesis, we postulated that enrichment for the protein may be a property of tumors.

To determine if uptake of MT-binding radionuclides increased in tumors, we measured uptake of Cd-109 (known to be highly bound to MT in biological tissues) in normal tissues and tumors grown from cultured cells in mice To verify that the Cd-109 was bound to MT, Sephadex G-75 ion-exchange chromatography of cytosolic extracts of tumor and liver was performed. We also compared the uptake of Cd-109 in-vivo tumors grown from four related cell lines which degree of expression of transformation.

Uptake of Cd-109 by the tumors exceeded that by normal tissues examined, with the exception of liver and kidney (the organs known to be richest in MT). The tumor:background ratios of activity were greater for Cd-109 than for Gallium-67 for most of the normal background tissues examined. Ion-exchange chromatography demonstrated that 90% of the activity in liver, and 75% of the activity in the tumors was associated with a low molecular weight fraction corresponding to that expected for MT. The magnitude of uptake of Cd-109 by tumors from four related cell lines parallelled their degree of expression of the transformed, or "malignant" phenotype. We conclude that metals which bind to MT may be useful for imaging or radiotherapy of cancer.

Posterboard 1257

BLOOD BRAIN BARRIER (BBB) STUDIES OF PATIENTS WITH PRIMARY BRAIN NEOPLASMS USING POSITRON EMISSION TOMOGRAPHY (PET).

R.J.Ott,M.A.Flower,J.W.Babich,P.Marsden,S.Webb, S.Cherry,V.R.McCready,A.Irvine,Royal Marsden Hospital Sutton,Surrey,UK

Prognosis for adults with primary brain neoplasms is poor and it is likely that several physiological factors play a role in efficacy of radiotherapy and chemotherapy.The permeability of the blood brain barrier is often affected by the neoplasm initially and again by the treatment and may seriously modify attempts to control or retard tumour growth. Quantitative dynamic PET imaging with a multiwire proportional chamber PET camera is to be used to measure BBB permeability before and after treatment of patients with primary brain tumours.100-150 MBq of Ga-68-EDTA is injected and 6-8 five min. tomographic studies acquired. Each image consists of 64x64x64 6mm pixels.A separate image of a venous blood sample is used to calibrate the concentration of the tracer in the patient images. The reproducability of these measurements is being determined from repeat studies several days apart on patients undergoing no treatment.Tracer washout curves obtained from region of interest analyses of these images indicate that measurements are repeatable to within 5-10%.From these data it is possible to make estimates of the influx and outflux constants from different parts of the brain as well as the plasma vascular volumes of these tissues. Measurements of changes in these parameters may enable quantification of changes in BBB permeability brought about by treatment and allow an evaluation of whether subsequent treatments will be of value.

Iannotti et al 1987,11(3):390-397.JCAT.

Posterboard 1258

TUMOR SCANNING WITH IN-111 DIHEMATOPORPHYRIN ETHER.

M.R. Quastel, A.M. Richter, D.M. Lyster and J.G. Levy. Univ. British Columbia and TRIUMF, Vancouver, BC, Canada and Ben Gurion Univ. of the Negev, Beer Sheva, Israel.

Dihematoporphyrin ether (DHE), the tumor localizing fraction of hematoporphyrin derivative (HPD), was radiolabeled with In-111 (Lavallee and Fawwaz,1986). The complex moved on TLC with an Rf≠0.8, just slower than the main fluorescent photopeak, using an ethanol: ethylacetate:water:ammonium hydroxide solvent. Unbound In-111 (In*) was reduced to 2-5% by passage through silica gel using the same solvent. DBA/2J mice hosting transplanted rhabdomyosarcomas (M1, methylcholanthrene-induced) were injected iv with In*DHE, and with In*-chloride as control. Within 1-2 hrs, both agents were taken up prominently by the tumors, liver, spleen and kidneys. After 24 hrs, the largest conc of In* (given as chloride) was found in the kidneys. In contrast, the liver took up most of the In*DHE. The tissue distribution of In*DHE was strikingly similar to that reported by Gomer and Dougherty (1979) for C-14- and H-3-HPD. Unlike In*chloride, 2/3 of the In*DHE cleared from the tissues within 24h. However, the tumor content showed much less fall off, thus resulting in a higher tumor:tissue ratio for the In*DHE treated mice. Tumor In*DHE at 24h was tested to assess the degree of separation of In* from the DHE in vivo. 0.15M acetic

acid/ethyl acetate extraction showed that 70 ± 8% of the In* remained associated with DHE, whereas the remainder of the In* did not move with solvent on TLC, as also observed for tumor extracts of mice given In*chloride. It is concluded that In*DHE has the same in vivo distribution and localization as HPD, and that it may be useful as a tracer for the quantitative assessment of DHE uptake in tumors during photodynamic therapy.

Posterboard 1259

PHARMACOKINETICS OF IN-111 2A11 (ANTI-GRP) MURINE MONOCLONAL ANTIBODY. N Shuke, JL Mulshine, JC Reynolds, I Avis, K Fujimori, Y Sawada, B Merchant, SM Larson, J Weinstein and JA Carrasquillo. National Institutes of Health; Bethesda, Md; and Hybritech, San Diego, Ca.

Using data from 8 patients (pts) with lung cancer, we evaluated the pharmacokinetics in serum and liver of In-111 2A11. 2A11, a murine monoclonal IgG1 directed at GRP, an autocrine growth factor, was labeled with In-111 using kits containing approximately 5 mCi and 2 mg. A mean of 89% of the In-111 was bound to the 2A11, with good retention of immunoreactivity. We performed a dose escalation trial using fractionated doses given 3 times a week for 4 weeks. Initially all pts received one kit mixed with unlabeled 2A11 (i.v.): 4 pts 1 mg/m^2; 3 pts 10 mg/m^2; and 1 pt 100 mg/m^2 (to date). Four pts received 2 doses of In-111 2A11 separated by 2 to 3 weeks. Plasma data and liver region of interest data from scintigrams (up to 7 days) were fitted to a linear 2 compartment model using a non-linear least squares regression program on an IBM/AT. Systemic and plasma clearance were determined also analyzed were hepatic clearance, elimination rate constant for liver and the volume for non-specific liver binding. Patients whose serum did not complex with 2A11 (by HPLC) had similar serum clearance and similar liver uptake that was independent of the dose of 2A11. In the absence of complex formation (in serum) patients receiving a second dose of antibody had kinetics similar to those predicted from the first dose. The pts with the highest complex formation in serum had the highest accumulation of activity in the liver. Our model suggests that for doses of 1 - 100 mg/m^2 of 2A11 there was no dose dependency in plasma or liver.

Posterboard 1260

MONOCLONAL ANTIBODY IMAGING USING IN-111-LABELED B72.3 IN HUMAN NON-SMALL CELL LUNG CARCINOMA (NSCLC). W.G. Spies, A.M. Zimmer, P.G. Robinson, J. LoCicero, J.A. Radosevich, E.H. Kaplan, A.B. Canude, L. Munzel, S.M. Spies, R.T. Maguire and S.T. Rosen. Northwestern University Medical Center, Chicago, IL and Cytogen Corp., Princeton, NJ.

Pre-operative imaging of 6 patients with biopsy proven NSCLC was performed after IV infusion of 2-5 mCi of In-111 B72.3 (0.2mg) monoclonal antibody (Cytogen Corp). All patients were surgical candidates and had not received any therapy within 4 weeks of the study. Biopsies of tumor and normal tissue were performed within 3-8 days of imaging. Whole body and plasma clearances ranged from 2.4-8.4 days and 15-52 hours respectively. Gamma camera images of the head, chest, abdomen and pelvis were obtained at 2 hours and at 1-4 days. SPECT images of the chest and/or abdomen were obtained in 4 patients. Early images demonstrated prominent blood pool activity. On later images, faint bone marrow and colonic activity was noted. Uptake in the primary tumor was visible in 3 patients and questioned in a fourth. Tumor/blood and tumor/normal lung ratios in these patients ranged from 1.2-4.0 and 3.8-5.0 respectively. Both patients without visible tumor uptake were negative for the antigen on immunoperoxidase staining. Other foci of focal chest uptake were noted in 3 patients, and focal paraaortic or other nodal uptake was seen in 4. A 7th patient imaged with 2 mg total antibody injected demonstrated better tumor visualization. Imaging of human non-small cell lung carcinoma with In-111 B72.3 monoclonal antibody is feasible and may be useful in the evaluation of these patients.

Posterboard 1261

BIODISTRIBUTION & BLOOD CURVES OF 2 MURINE MONOCLONAL ANTIBODIES (MoAb) IN MELANOMA PATIENTS (PTS). G. Vahjen, E. Cornelius, S. Zoghbi, R. Neumann, J. Kirkwood, M. Ernstoff, G. Zubal, Yale Medical School, New Haven, CT

27 pts were given 1-40 mg of ZME-018 MoAb (Z) tagged with In-111-DTPA; 26 received 20 mg of 96.5 MoAb. Serial blood samples were drawn from Z pts. Both groups were imaged by gamma camera with computer data storage. Z showed ↑ blood $T_{1/2}$ with dose. At 1 & 2.5 mg, blood curves were triphasic; above this, the curves showed a single phase with ? of a short first phase. Data on 96.5 from the literature (Murray J, et al; Halpern S, et al) was also analyzed with our data. Organ: heart (blood) ratios were standardized by correction for blood level changes with time and dose, thus permitting comparisons of organ activity. Both MoAbs distributed widely, but mainly in liver, spleen, marrow and bowel. [Z] > [96.5] in spleen, bone, testis, bowel, lung, mouth & axilla but < in liver. Both MoAB showed little Δ in distribution with time (excluding blood) but marked Δ with dose. Low dose 96.5 showed high liver uptake with a biphasic ↑ with dose. Low dose Z showed high spleen and marrow uptake with a biphasic ↑ with dose. Both suggest saturation of high affinity sites. Z also showed a biphasic ↑ in blood, bowel & lung, with a gradual liver ↑ . Multiple mechanisms appear involved.

Posterboard 1262

CORRELATION OF IN-111 ANTI-CEA MONOCLONAL ANTIBODY IMAGING WITH SURGICAL FINDINGS IN PATIENTS WITH COLORECTAL CANCER. D. Yamauchi, L. Williams, B. Morton, D. Beatty. City of Hope National Medical Center, Duarte, CA.

Thirty patients (pts) with known or suspected primary (1°) or metastatic (2°) colorectal cancer (CrCa) underwent scintigraphy (Scnt) with In-111 ZCE-025 (ZCE) anti-CEA antibody (Hybritech). Pts received 20 or 40 mg. of ZCE labeled with 2.5 to 6.5 mCi of In-111. Scnt of the torso was obtained up to 7 days following injection. Scnt was correlated with preoperative radiographic studies (i.e. BE, CT, and US) as well as results of surgery performed within the following 21 days.

1° CrCa was seen in 22 pts, hepatic 2° CrCa in 10 pts, extrahepatic 2° CrCa in 10 pts. In 27 of these pts, 44 ZCE-avid lesions were identified. Three pts had no lesions imaged. Forty of these sites were pathologically examined and in 78% (31/40), CrCa was documented.

Of 10 pts with proven hepatic 2° CrCa, only 1 had a ZCE-avid lesion (3 others had cold lesions). Thus, 30 of 31 had extrahepatic sites. Four were at or above the diaphragm. For extrahepatic lesions > 2 cm, there were 7 false negatives (FN) and 9 false positives (FP). Using these criteria, sensitivity was 82% (31/38) and predictive value of a positive site was 78% (31/40). FP images resulted largely from uptake in histologically normal lymph nodes draining the 1° or 2° tumor. FN images tended to occur in lesions that were small, had low CEA content or were located in the lungs.

In conclusion, In-111 anti-CEA Ab imaging is effective and reliable in localizing 1° and 2° extrahepatic CrCa. This technology complements other imaging modalities and is useful in CrCa pt management.

Pulmonary

Posterboard 1263

TECHNETIUM UP-SCATTER IN KRYPTON VENTILATION IMAGES. K. Levin, W.J. Slizofski, S. Dadparvar. Hahnemann University Hospital, Philadelphia, Pa.

In our institution, we perform ventilation scans with Krypton-81m following the perfusion images which are performed using Technetium-99m MAA. We recently became aware of an artifact caused by the up-scatter of Technetium-99m into the Krypton-81m window (20% centered at 191 Kev). We have been unable to find any previous reports of this phenomenon. A preliminary investigation of 11 patients to assess the magnitude of the up-scatter showed that the percentage of counts in the Krypton image from Tc99m varied from 2% to 27%. This artifact is a very low resolution image of the Tc99m-MAA scan. This is superimposed on the Krypton image. We are uncertain if this artifact is clinically significant, but want those who perform ventilation scans with Krypton-81m to be aware of this artifact.

Posterboard 1264

DELAYED LUNG SCINTIGRAPHY WITH N-ISOPROPYL-I-123-p-IODOAMPHETAMINE IN LUNG CANCER AND INFLAMMATORY DISEASE. T.Suematsu,I.Narabayashi,Y.Takada,K.Ohbayashi,and T.Komiyama. Hyogo Medical Center for Adults, Akashi, Japan.

Lung studies with N-Isopropyl-I-123-p-Iodoamphetamine(IMP) were performed on 29 patients with lung cancer (34 lesions), 3 with radiation pneumonitis, 2 with interstial pneumonia, 1 with diffuse panbronchiolitis, 1 with bronchopneumonia, 1 with lung abscess and 1 with old tuberculous lesion of the lung. Early and delayed scintigraphy practiced immediately and 24 hr after administration of a dose of 3 mCi of IMP. In present study, we evaluated the significance of the delayed scintigraphy. No difinite trend caused by difference in histological types of cancers was recognized. There was no IMP uptake congruent with the tumor in 24 lesions. In 22 lesions out of 24, high IMP uptake was seen on the periphery of the tumor. On the other hand, no significant change was recognized in 8 lesions, whose sizes were small. Therefore, it seemed that high IMP uptake was related to the inflammation and/or the atelectasis surrounded the tumor.

In 8 patients with viable inflammatory disease of the lung, the delayed scintigram showed high IMP uptake congruent with the lesion. No uptake was seen in the old tuberculous lesion.

The delayed lung scintigraphy with IMP is very useful for differentiation between lung cancer and inflammatory disease of the lung.

Radioassay

Posterboard 1265

IODINE-124 : A UNIQUE DUAL LABEL FOR DIAGNOSTIC (PET) AND THERAPEUTIC RADIOPHARMACEUTICALS. R.M. LAMBRECHT, M. Sajjad and S. Bakr. King Faisal Specialist Hospital and Research Centre, Radionuclide & Cyclotron Operations Department, Riyadh, Kingdom of Saudi Arabia

Iodine-124 ($t_{\frac{1}{2}}$ - 4.16 d, β^+= 25%) has appropriate physical characteristics for its novel use in certain radiopharmaceuticals that can be utilized at low dose for PET diagnostic evaluation of physiologic function, anatomic determinations, etc.; and at high dose for radiotherapy. The primer motivation is application of I-124 in monoclonal antibodies (MAb) as radioimmunospecific agents. The cyclotron parameters and radiochemistry for production of 99.8% radionuclidic purity (I-124) via the Te-124 (d,2n) reaction is now developed. I-126 is the radionuclidic impurity. Yields of 300 mCi are obtained at 40 h post-irradiation, with a production rate of 0.55 ± 0.05 mCi/μAh utilizing 50-90 μA of 15 MeV D^- on electroplated T-124 internal targets of 13 ± 0.5 mg cm^{-2} of 94% isotopically enriched Te-124. 100mCi reductant-free I-124 solutions at pH 9.0 undergo ~20% autoradiolytic decomposition in 9 d. Extensive radioanalytical studies established conditions to preserve the I-124 (in the absence of $Na_2S_2O_3$ reducing agent) as 99% iodide for labeling. I-124 was developed for incorporation into radioimmunospecific radiopharmaceuticals, and for labeling m*-IBG for the evaluation of pheochromocytomas and neuroblastoma. Iodide-124 was used in an earlier PET study of a patient with thyroid carcinoma. The radioassay quantitation afforded by PET should lead to more effective dose determination in radiotherapy, and also be predictive of the efficiency of treatment with radioiodine labeled radiopharmaceuticals.

Radiopharmaceutical Chemistry

Posterboard 1266

ALTERED BIOROUTING OF RADIOPHARMACEUTICALS DUE TO INTERFERENCES WITH SELECT PHARMACEUTICAL AGENTS. D.L. Laven, S.J. Harwood, P.J. Goldner, G.J. McNulty, and S.T. DeRuzzo. Veterans Administration Medical Center, Bay Pines, Fl.

Drug-radiopharmaceutical interactions and Pharmacologic interventions have become two increasingly important concepts within nuclear pharmacy and nuclear medicine practice. However, little is known concerning the clinical frequency with which select examples of drug-radiopharmaceutical interactions occur. As part of an on-going research effort, we present findings on the clinical frequency of select examples of previously reported drug-radiopharmaceutical interactions, as noted in our patient screening program. This program is based on prospective review of patient medical data bases, and has included more than 891 outpatient and 3244 inpatient imaging studies.

Four different types of imaging procedures were looked at initially: Lung studies (using Tc99m-MAA and Xe-133 gas); Liver/Spleen studies (using Tc99m-Albumin Colloid); Bone studies (using Tc99m-MDP); and Tumor/Abscess studies (using Ga-67 citrate). Extensive literature review was the basis for establishing the screening list of drug agents suspected of interfering with radiopharmaceuticals A preliminary analysis of our data shows that there are predictable examples whereby an altered biorouting of a radiopharmaceutical can be attributed to a drug agent, such as: 7 of 18 drug agents identified for lung studies; 14 of 41 drug agents identified for liver/spleen studies; 21 of 38 drug agents identified for bone studies; and 22 of 69 drug agents identified for tumor/abscess studies.

Posterboard 1267

THE SYNTHESIS OF SEMI-RIGID POLYAMINOCARBOXYLATES AS NEW BIFUNCTIONAL CHELATING AGENTS. R.C. Mease, S.C. Srivastava, Brookhaven National Laboratory, Upton, NY.

The aim of this study is to prepare new chelating ligands with the potential of forming more stable metal complexes and antibody-chelate-metal conjugates. Our approach is to substitute a rigid molecule such as trans-1,2-diaminocyclohexane for an ethylene diamine portion of a polyaminocarboxylate. The rigidity of the

cyclohexane ring fixes two of the nitrogens into a position where they can readily complex metals. This effect is observed in the 10- to 1000-fold increase in the stability constants of cyclohexyl EDTA (CyEDTA)-metal complexes compared to EDTA. We have prepared the dianhydride of CyEDTA (CyEDTADA) by the room temperature reaction of commercial CyEDTA with acetic anhydride and pyridine. A 5/1 CyEDTADA/IgG molar ratio in 0.1 N $NaHCO_3$ at a protein concentration of 15 mg/ml conjugated an average of 3 CyEDTA molecules/IgG.

The cyclohexyl derivates of DTPA and TTHA have been synthesized starting with N-tert-butyloxycarbonyl-trans-1,2-diaminocyclohexane and trans-1,2-diaminocyclohexane, respectively. To each of the starting compounds, the ethyleneamine portion(s) was added by acetylation with isobutylchloroformate and N-(tert-butyloxycarbonyl) glycine, followed by hydrolysis of the tert-butoxycarbonyl groups and borane reduction of the amide. Amine alkylation with bromoacetic acid resulted in the desired compounds. Antibody labeling with radiometals using these ligands is in progress.

Work supported under U.S. Department of Energy Contract No. DE-AC-76CH00016.

Posterboard 1268

Identification of the Major Urinary Metabolites of Para-Iodobenzoate Conjugates of an Antibody Fragment in Humans: Comparison with Chloramine-T. D.B. Axworthy, D.S. Wilbur, R.W. Schroff, S.W. Hadley, M.D. Hylarides, C. Collins, W.B. Nelp, and A.R. Fritzberg. NeoRx Corporation and University of Washington, Seattle, WA.

An investigation of the application of radioiodinated monoclonal antibodies to the therapy of melanoma is underway. Radioiodinated antibodies produced by two separate labeling methods are being studied by coadministration of I-131 and I-125 labeled antibody. The objective of the coinjection was to compare the in vivo characteristics of the antibody labeled with para-iodobenzoate (PIP) with the conventional method of chloramine-T (ChT) labeling. PIP labeling of antibodies has been developed to obtain radioiodinated antibodies which are resistant to in vivo deiodination (JNM 1986;27,959). Two patients recieved NRML-01 $F(ab')_2$ labeled with PIP I-125 (1 mCi) and ChT I-131 (7 mCi). One patient recieved NRML-01 $F(ab')_2$ PIP I-131 (7 mCi) and ChT I-125 (1 mCi). The total urinary output of each patient was collected over 4 days. The urine samples from 22-23 time points were collected separately, counted, filtered through a 10,000 dalton pore size membrane, and injected into a HPLC system. Reverse-phase HPLC analysis of the filtrate (>90% of the radioactivity) indicated that the major metabolites for the PIP labeled antibody were the lysine adduct (>80%) and the glycine adduct (>10%) of para-iodobenzoic acid. The major urinary metabolite of ChT labeled $F(ab')_2$ was iodide (>80%). Confirmation of the radioiodide was obtained by treating the urine filtrate, which had iodide added, with silver nitrate to form an insoluble silver iodide (iodate or periodate) precipitate. The precipitate was centrifuged, separated from the urine, and washed repeatedly. The precipitate confirmed the HPLC findings with over 80% of the activity being found in the pellet. Silver nitrate treatment of radioiodinated benzoate did not precipitate any of the radioactivity. In summary, the major urinary metabolites of PIP labeled NRML-01 $F(ab')_2$ appears to come from catabolism of the protein. ChT labeled NRML-01 $F(ab')_2$ yielded almost exclusively free iodide, iodate, or periodate as the major urinary metabolites. (Supported in part by PHS grant #CA-29639)

Posterboard 1269

SYNTHESIS, REACTIONS AND APPLICATIONS OF [^{11}C]-THIOCYANATE: ALI M. EMRAN, POSITRON DIAGNOSTIC AND RESEARCH CENTER, UNIVERSITY OF TEXAS HEALTH SCIENCE CENTER, HOUSTON, TX.

There are several [C-11]-labelled compounds which can be produced directly from [C-11]-thiocyanate or via [C-11]- thiourea. Thiourea is an important intermediate in a number of synthetic schemes which will end up in producing pharmacologically active compounds. Thiopyrimidines such as thiopental, thiazoles such as 2-aminothiazole and thiouracils such as thiouracil or propylthiouracil are examples of such compounds. Thiopental is used as an anesthetic. 2-Aminothiazole is a thyroid inhibitor. It is produced via thiourea in a reaction with 1,2-dichloroethyl acetate. Thiouracil is used for treatment of hyperthyroidism, angina pectoris and congestive heart failure. It is prepared by condensing thiourea with ethyl formylacetate. Propylthiouracil is also used as a thyroid inhibitor and is prepared by reacting ethyl ß-oxocaproate with thiourea. The synthesis of [C-11]-thiocyanate has been carried out in solution by heating [C-11]-cyanide with sulfur. It was used further for the synthesis of [C-11]-thiourea by addition of excess ammonium sulfate followed by thermal transformation of the produced ammonium thiocyanate. The yield is quantitative and the reactions are completed in approximately 30 minutes from EOB. Utilization of the prepared [C-11]-thiourea as a synthone in the above reactions is under further investigation.

Posterboard 1270

FACILE SYNTHESIS OF CARBON-11 LABELLED BUPRENORPHINE FOR PET STUDIES OF OPIATE RECEPTORS. J. R. Lever, S. M. Mazza, R. F. Dannals, H. T. Ravert, A. A. Wilson, J. J. Frost and H. N. Wagner, Jr. The Johns Hopkins Medical Institutions, Baltimore, MD.

Buprenorphine (BPN), a potent partial agonist, is a clinically used analgesic (Temgesic) which exhibits pharmacokinetic properties suitable for *in vivo* studies of opiate receptors. We have synthesized [11-C]-BPN using methodology similar to that employed for the preparation of the structural congener, [11-C]-diprenorphine (Lever *et al.*, Tetrahedron Lett., 28, 4015, 1987). The precursor 1 was prepared in two steps with an over-all yield of 84% by treatment of BPN with $LiAlH_4$ / CCl_4 to provide 6-desmethyl-BPN followed by protection of the phenolic hydroxyl as the *t*-butyldimethylsilyl ether. Treatment of 1 with NaH in DMF containing CH_3I for 3 minutes at 80 °C resulted in selective 6-O-methylation and desilylation to give a sample which displayed spectral and chromatographic characteristics identical to those of authentic BPN. For radiosynthesis, [11-C]-CH_3I carried by a stream of N_2 was trapped at -78 °C in a solution of 1 (2.0 mg) in DMF (0.2 mL). The mixture was transferred to dry NaH (3.5 mg), heated at 80 °C for 2 minutes and then quenched (1.0 N HCl, 0.15 mL). Purification by reverse-phase HPLC, concentration and formulation provided a sterile, pyrogen-free solution of [11-C]-BPN . The synthesis, isolation and formulation required 20 minutes from E.O.B. At E.O.S., the radiochemical yield was 10% based on [11-C]-CH_3I, while the specific activity was 1425 mCi/µmol. Studies with [11-C]-BPN should help define dose-response and subsite occupancy relationships for a variety of opiate ligands *in vivo* by PET.

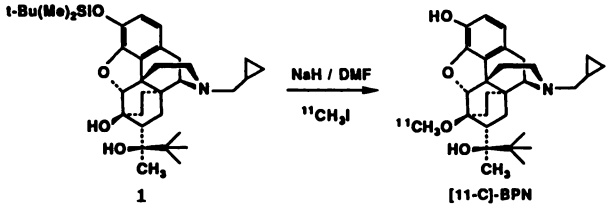

Posterboard 1271

SYNTHESIS OF [C-11] LABELED TAMOXIFEN VIA REDUCTIVE CARBOXYLATION. S. Ram, R.E. Coleman and L.D. Spicer, P.E.T. Facility/Nuclear Medicine, Duke University Medical Center, Durham, NC

Tamoxifen 1-[4-(2-dimethylaminoethoxy)phenyl]-1,2-diphenyl-1-butene is a non-steroidal, antiestrogenic drug used widely in the treatment of human breast carcinomas. In our efforts to develop fast and efficient methods for [C-11] labeled radiopharmaceuticals using CO_2 directly as a radiolabeled precursor, we have investigated reductive-carboxylation in the synthesis of this compound. A method using [C-11] methyl iodide has previously been reported. In our approach, reaction of CO_2 with the N-TMS derivative of dismethyltamoxifen gave the trimethylsilylcarbamate derivative which following in situ reduction with 35% solution of sodium bis (2-methoxyethoxy) aluminum hydride in toluene at 65 ± 5°C for 10 min afforded impure tamoxifen. Inter-

mediates in the reaction as well as products were identified by ^{1}H NMR, TLC and HPLC during synthesis with [C-12] CO_2. Final purification over a basic alumina Sep-pak cartridge using ethyl acetate: methanol:58% NH_4OH (9:0.9:0.1) gave pure tamoxifen in 75% yield for the exploratory C-12 synthesis. It should be noted that this method has previously been found by us to be useful in the presence of a wide variety of labile functionalities and in this case gives excellent results without affecting the carbon-carbon double bond. In a radiochemical synthesis using [C-11] CO_2 as the labeling reagent, N-[C-11] methyl tamoxifen was obtained in 65% radiochemical yield (EOB) and > 99% radiochemical purity.

Posterboard 1272

Identification of the Major Urinary Metabolites of Para-Iodobenzoate Conjugates of an Antibody Fragment in Humans: Comparison with Chloramine-T. D.B. Axworthy, D.S. Wilbur, R.W. Schroff, S.W. Hadley, M.D. Hylarides, C. Collins, W.B. Nelp, and A.R. Fritzberg. NeoRx Corporation and University of Washington, Seattle, WA.

An investigation of the application of radioiodinated monoclonal antibodies to the therapy of melanoma is underway. Radioiodinated antibodies produced by two separate labeling methods are being studied by coadministration of I-131 and I-125 labeled antibody. The objective of the coinjection was to compare the in vivo characteristics of the antibody labeled with para-iodobenzoate (PIP) with the conventional method of chloramine-T (ChT) labeling. PIP labeling of antibodies has been developed to obtain radioiodinated antibodies which are resistant to in vivo deiodination (JNM 1986;27,959). Two patients received NRML-01 F(ab')$_2$ labeled with PIP I-125 (1 mCi) and ChT I-131 (7 mCi). One patient received NRML-01 F(ab')$_2$ PIP I-131 (7 mCi) and ChT I-125 (1 mCi). The total urinary output of each patient was collected over 4 days. The urine samples from 22-23 time points were collected separately, counted, filtered through a 10,000 dalton pore size membrane, and injected into a HPLC system. Reverse-phase HPLC analysis of the filtrate (>90% of the radioactivity) indicated that the major metabolites for the PIP labeled antibody were the lysine adduct (>80%) and the glycine adduct (>10%) of para-iodobenzoic acid. The major urinary metabolite of ChT labeled F(ab')$_2$ was iodide (>80%). Confirmation of the radioiodide was obtained by treating the urine filtrate, which had iodide added, with silver nitrate to form an insoluble silver iodide (iodate or periodate) precipitate. The precipitate was centrifuged, separated from the urine, and washed repeatedly. The precipitate confirmed the HPLC findings with over 80% of the activity being found in the pellet. Silver nitrate treatment of radioiodinated benzoate did not precipitate any of the radioactivity. In summary, the major urinary metabolites of PIP labeled NRML-01 F(ab')$_2$ appears to come from catabolism of the protein. ChT labeled NRML-01 F(ab')$_2$ yielded almost exclusively free iodide, iodate, or periodate as the major urinary metabolites. (Supported in part by PHS grant #CA-29639)

Posterboard 1273

YTTRIUM-90 LABELLED ANTIBODIES: THE INFLUENCE OF DTPA ON DOSE DISTRIBUTION. A.P.H. Farnsworth and A.T.M. Vaughan. Immunology Dept, Birmingham University, Birmingham, U.K.

Cyclic DTPA anhydride conjugated antibodies labelled with Y-90 were assessed for stability both in-vitro, and in-vivo in a nude mouse tumour model. The effect of DTPA administration on the radiolabel biodistribution was also measured. Immunoreactivity was 70%, as shown by an ELISA and histochemistry. In-vitro, dialysis showed the label to be stable over a pH range of 10.2 to 5.4, independent of the buffer used. Below pH 4.5, label was rapidly lost. Use of Sephadex G25 chromatography following incubation of the DTPA-Y-90 complex in human serum, transferrin or albumin, showed the activity to be lost at 1.8% per day in serum and transferrin, but <0.5% per day in albumin.

For in-vivo work, mice bearing human colon carcinoma xenografts received i.p. injections of labelled antibody and were sacrificed at various time intervals. One group of mice received a series of DTPA injections 48 hrs post-antibody injection, and were analysed 24 hrs later with a control group. Tumour localisation was observed, but high levels of Y-90 were also seen in liver, kidney and bone. At 4 days, the activity (%I.D./g) in all tissues studied was significantly reduced after the DTPA treatment.

	Liver	Kidney	Bone	Tumour
Controls	5.48±1.49	4.55±0.30	4.96±1.08	11.12±1.75
Treated	2.77±0.36	1.98±0.85	2.94±0.23	5.54±1.19

The ability of DTPA to remove Y-90 from tissue implies that this Y-90 is located extra-cellularly and unbound to chelate or antibody. This may result from either enzymatic processing of the antibody or dissociation from the complex due to low pH. If DTPA can be used to reduce the dose to non-tumour locations only, the procedure may then be of use in tumour therapy using Y-90.

Posterboard 1274

Tc-99m Sn-ANTIMELANOMA F(ab')$_2$: CHANGES IN CHEMICAL AND RADIOCHEMICAL COMPOSITION. Gy.A.Jánoki,L.Kőrösi,B.Spett, L.Csernay* "FJC" Nat.Res.Inst.for Radiobiology and Radiohygiene, Budapest P.O.Box 101.1775, Hungary
* A.Szent-Györgyi Medical University, Szeged, Hungary

Clinical observations suggested that the composition and stability of a Tc-99m(Sn) antimelanoma F(ab')$_2$ fragment freeze-dried with HSA may change with time. We performed direct study to determine the chemical and radiochemical composition of this radiopharmaceutical. Standard PAGE, HPLC and electroimmunoassay (EIA) were used for analysis during storage before and after labelling. HPLC analysis of antibodies was performed with a BIO-RAD HPLC system. Chromatographic separation was carried out by using a 300 x 7.5 mm Bio-Sil TSK-250 column. Samples were eluted with 0.02 M NaH_2PO_4/0.05 M Na_2SO_4buffer at pH 6.8 at a flow rate of 1.0 ml/min. Absorbance (280 nm) and gamma radiation were measured with a flow-through detector. Peaks in HPLC were identified through the injection of standards with molecular weights near to that of the component to be determined. Two HPLC peaks were generally observed. More than 90 % of the activity was associated with the first peak /F(ab')$_2$/. The radioactivity distribution after storage or in the case of a preparation labelled near to the expiry date was changed significantly: 90 % of the label peak was then associated with the second peak /F(ab') + HSA/. Specific EIA was used to measure the label transfer to HSA. The measurements yielded a value of 5-15 %, which did not explain the activity rise in the second peak. It is concluded that the F(ab')$_2$ fragment containing Sn(II) splits to the F(ab') fragment with unknown kinetics. The mixture of two fragments exhibits variable bio-distribution and kinetics in clinical studies.

Posterboard 1275

TUMOR TARGETING COMPARISON OF ANTI-CARCINOEMBRYONIC ANTIGEN (CEA) MONOCLONAL ANTIBODY (MAb) COUPLED WITH FIVE DIFFERENT DTPA-DERIVATIVES. C. Motta-Hennessy, R.M. Sharkey, O.A. Gansow, I. Fand, M. Eddrey, and D.M. Goldenberg. CMMI, NIH.

An anti-CEA MAb, NP-4, was coupled to 5 derivatives of DTPA at a ratio of 1-2 DTPA/MAb. The cyclic anhydride (CA) derivative was compared to 4 other DTPA derivatives that used the isothiocyanate (ITC) function for coupling to MAbs. The other derivatives were: ITC-Bz-DTPA, 1M3B-DTPA, 1B3M-DTPA, and Mx-DTPA (M=Methyl; B=p-isothiocyanate-benzyl; Mx:50% 1M3B; 50% 1M4B). Conjugates were prepared with all the compounds without alteration in physical or immuno-chemical properties of the MAb. These MAb conjugates were labeled with In-111 at a specific activity of 6 mCi/mg, and were then injected into nude mice bearing colonic tumor xenografts. All of the ITC-derivatives had similar tumor localization properties with respect to the percent uptake in the tumor (30-40%/gram on day 3), blood clearance rates, and tumor/non-tumor ratios. In comparison, animals given the In-111-labeled CA-DTPA conjugated MAb showed a 2-3 fold faster blood clearance rate, a 4-5 fold decrease in tumor uptake, and 2-3 times higher liver uptake indicating that the MAb coupled to CA was significantly inferior to the ITC-DTPA derivatives for tumor

localization. We are evaluating the suitability of these derivatives for Y-90-NP-4 therapy in animals. Preliminary data suggests that there is appreciable Y-90 uptake in the bone and this may limit the utility of this method.

Posterboard 1276

SYNTHESIS AND CHARACTERIZATION OF CRYPTATES AS POTENTIAL RADIONUCLIDES CARRIERS IN RADIOIMMUNOTHERAPY. W.A. Pettit, Y. Iwai, B. Swailes, and C.F. Barfknecht. V.A. Medical Center and University of Iowa, Iowa City, IA.

The objective of this study is to develop and evaluate a model system of cryptate/antibody conjugates for radioimmunotherapy. Cryptates are 3-sided cage structures of ethoxy ether linkages between two bridgehead nitrogen atoms. Our chemical synthesis and characterization of 4,7,13,16,21,24-hexaoxa-5,6-(4'aminobenzo)-1,10-diazabicyclo[8.8.8]hexacosane, $2BNH_2$:2:2, provides a compound which can be chemically modified for facile conjugation to proteins or more specifically, antibodies to tumor antigen. Commercially available 4,7,13,16,21,24-hexaoxa-5,6-benzo-1,10-diazabicyclo[8.8.8]hexacosane,2B:2:2, has been used to examine the formation and stability of its Ba-133 complex. The radionuclide/cryptate complex which was produced in refluxing acetonitrile was isolated by solvent evaporation and extraction into methanol. High performance liquid chromatography (HPLC) and thin layer chromatography (TLC) have been used to characterize the 2B:2:2 + Ba^{+2} $\rightleftharpoons$ 2B:2:2/Ba^{+2} complex system. Reverse phase HPLC in methanol and acetonitrile has been used to distinguish 2B:2:2 and its Ba^{+2} complex. Retention volumes are 3.5 and 1.2 ml in methanol and 5.2 and 1.6 ml in acetonitrile, respectively. In addition, TLC on silica gel using 4:4:1 acetonitrile:water:1% aqueous acetic acid delineates 2B:2:2/Ba^{+2}, and free Ba^{+2}. Preparation of the isothiocyanate derivative of $2BNH_2$:2:2 affords a convenient means of protein attachment and will stimulate consideration of alternative radionuclides for radioimmunotherapy.

Posterboard 1277

THE IMMUNOREACTIVE FRACTION OF MONOCLONAL ANTIBODIES AGAINST OVARIAN CARCINOMA AFTER LABELLING WITH In-111 AND I-125. *K. Sheldon, +R. Reilly, *A. Marks, +S. Houle *University of Toronto and +Toronto General Hospital, Toronto, Ontario, Canada.

This study was carried out to determine the immunoreactive fraction at infinite antigen excess (1) of monoclonal antibodies (McAb) 10B, 8C and M2A (specific for ovarian carcinoma) after labelling with In-111 and I-125. The McAb were labelled with In-111 using the cyclic DTPA anhydride method or with I-125 using chloramine-T. The substitution level of the In-111 McAb was 1.2-1.5 mols DTPA/mol McAb. The specific activity was 1-2 uCi/ug and the radiochemical purity was 80-90% (In-111 McAb) or > 95% (I-125 McAb).

The immunoreactive fraction was determined by measuring the binding of 10ng of radiolabelled McAb to serial dilutions of HEY cells (a human ovarian carcinoma cell line) ranging from 5×10^6 cells to 4×10^7 cells.

The mean immunoreactive fractions were:

In-111	10B: 0.21 ± 0.08	I-125	10B: 0.73 ± 0.21
	8C: 0.31		8C: 0.48 ± 0.22
	M2A: 0.17		M2A: 0.52

The results show that labelling these McAb with In-111 using the cyclic DTPA anhydride method caused a significant reduction in the immunoreactive fraction. Labelling with I-125 did not reduce the immunoreactive fraction to the same extent. These findings may have implications for the diagnostic or therapeutic use of these McAb.

1. Lindmo, T., Boven, E., Cuttitta, F. et al, J. Immunol. Meth. 72:77-89, 1984

Posterboard 1278

METHODOLOGY FOR TC-99M-HM-PAO PLATELETS LABELING
G. Demonceau, P. Ziegels, P. Rigo, M. Brasseur, M. Stegen, Y. Beguin, G. Fillet, J.L. David, R. Leclercq, J.C. Depresseux and P. Bourgeois (University of Liege, Bracops Hospital, Belgium)

We investigated differents conditions of incubation for the labeling of platelets with Tc-99m-HM-PAO

We studied the number of platelets in the incubation volume (initial whole blood of 65,43,22 or 10 ml), the time (between 2 to 120 minutes) the volume of incubation (2 to 5 ml) and varying amounts of lipophilic Tc-99m-HM-PAO (370,740 or 1110 MBq). The influence of the concentration of ACD (10-20 %) was also tested. Mean platelet span was studied in 5 healthy volunteers and elution in vitro was tested in plasma up to 48 hours after labeling.

Increasing the number of platelets and the time of incubation as well as decreasing the volume of incubation improve the labeling efficiency, but no influence was found for the amount of lipophilic Tc-99m-HM-PAO nor the concentration of ACD. We obtained a mean labeling efficiency of 55.4±7.4% using 43 ml of whole blood, 2.5 ml as incubation volume and 1 hour incubation time. ADP and collagen induced normal aggregability. Mean platelet span was 66.9± 20 hours, significantly lower than with In-111-chelates or Cr-51-chromate. It was due to some degrees to spontaneous elution of the tracer, as observed in vitro.

We have developed a easy-to-perform, daily available tool to study platelets deposits, but not to evaluate platelet survival.

Posterboard 1279

TECHNETIUM-99m LABELLING OF LEUCOCYTES FOR ABSCESS IMAGING. T.F. McLeod, T.E. Boothe, I.T. Lauredo and W.M. Smoak. Mt. Sinai Medical Center, Miami Beach, FL.

The purpose of this study was to evaluate the use of Tc-99m SnF colloid labelled leucocytes for scintigraphic localization of abscesses. Several investigators have reported the use of Tc-99m SnF colloid as an effective label for leucocytes. In order to evaluate rbc and wbc labeling, heparinized human blood was centrifuged and the buffy coat and an approximate equal volume of rbc from the bottom of the tube were each suspended in 3 ml of plasma. The buffy coat suspension contained 1.14×10^4 wbc/mm^3 and the rbc suspension <1 wbc/mm^3. Both were incubated with 20 MBq of Tc-99m SnF colloid (Schroth, et. al. Eur. J. Nucl. Med. 6:469-472, 1981) for 1 hour at 37°C. After two washes in plasma at 100xg, 54% of the activity remained in the wbc suspension and 10% in the rbc suspension. Sodium citrate(0.5%) was added and incubated for 45 min at room temperature. The activity in the buffy coat pellet was reduced by 17% and the rbc pellet by 18%. Imaging of an abscess with labeled leucocytes was evaluated in a rabbit. Rabbit leucocytes were labeled with Tc-99m SnF colloid(27.8 MBq/9×10^7 wbc) and infused intravenously into a rabbit with a turpentine induced abscess in the thigh. After 2 hours images indicated there was accumulation of activity in the abscess and by 18 hours the abscess was clearly visible. The ratio of abscess:blood was 332:1. These data further confirm that Tc-99m SnF colloid labels leucocytes and to a lesser extent rbc. Under these conditions most of the label was not solubilized suggesting that it is internal. The images obtained suggest that this method may be useful to locate abscesses.

Posterboard 1280

PREPARATION AND CHROMATOGRAPHIC STUDY OF Tc-99m-BIGUANIDE COMPLEXES. C.C. Yu and D.E. Tow. Brockton/West Roxbury VA Medical Center, Brockton, MA.

In an effort to develop new Tc-99m radiopharmaceuticals, we are reporting the preliminary results of chromatographic studies on the reaction of phenylbiguanide with Tc-99m.

Biguanide has been identified as a bidentate ligand for chelation with a series of metals (e.g. Ni, Cu, Ag) to give square coordination.[1] When Tc-99m pertechnetate was reduced by freshly prepared $SnCl_2$ solution in the presence of phenylbiguanide at room temperature for 30 min, the radiochromatographic profiles (ITLC-SG/ethyl acetate) of the crude reaction mixture displayed two distinctive peaks as major components (>85% in yield). These labeled materials exhibited a chemical stability at pH 7.0 for at least 15 hr and gradually underwent decomposition at higher pH (11-12) for the same time period. The labeled compounds can be extracted with ethyl acetate to give 90% of the radioactivity in yield and then separated by HPLC equipped with a C-18 reverse phase column and a mobile phase of methanol-water (85:15, 0.01M ammonium acetate, pH 7.1). Electrophoresis studies were performed with cellulose acetate and chromatographic paper strips in 0.05M phosphate (pH 7.0) at 200V for 30 min and at 350V for 10 min; no significant migration of labeled spot was observed in either medium.

Two isomeric structures of these Tc-99m complexes were proposed and the biodistribution studies are under investigation.

1. L. Fabbrizzi, M. Micheloni, and P. Paoletti. Inorg. Chem., 1978, 17, 494.

Posterboard 1281

THE USEFULNESS OF 123-I HIPPURAN FOR L/R RATIOS AND EVALUATION OF RENAL FUNCTION BY FACTOR ANALYSIS. D.G. Pavel, E. Olea, A. Bello, B. Patel, K. Zolnierczyk. University of Illinois Hospital, Chicago, IL; University of Chile, Santiago.

We have evaluated the clinical usefulness of I-123 Hippuran (123-H) in the context of functional image processing by Factor Analysis (FA) and for replacement of L/R ratios usually obtained with Tc-DTPA. Five normals and 10 patients were evaluated, using 800-1000 uCi 123-H. In 6/10 a 131-H study, at short interval, was also available. FA was performed by an algorithm based on the method previously described by Bazin and Di Paola. Each study was processed for intervals of 3, 5, 10, 20 minutes and compared, when available, with 131-H and Tc-DTPA of same subject, or with comparable cases. Results: The factor images and respective loading curves of 123-H were much less noisy in all cases. This was particularly appreciated for processing of 4 and 5 factors as is needed in subjects with very different dynamics, in each and within each kidney. The amount of counts was sufficient to enable even a 3 min processing (10 sec frames) for evaluation of L/R ratios. FA showed a much lesser amount of hepatic and/or splenic accumulation around kidneys, thus removing a major cause of variability of L/R ratios. In general cortex and ureters were very well delineated on the respective images. Conclusion: Due to better information density, 123-H enables superior FA results (up to 5 factors) with crisp images and well defined curves. In addition L/R ratios can be obtained over 3 min intervals, with less background-induced variability than for Tc-DTPA. Except for GFR, all the information needed can be obtained with a single radiopharmaceutical.

Posterboard 1282

PREDICTION OF TESTICULAR VIABILITY WITH RADIONUCLIDE SCROTAL IMAGING. E. Yeo, D.C.P. Chen, L.E. Holder and M.E. Siegel, Union Memorial Hospital, Baltimore, MD and LAC/USC Medical Center, Los Angeles, CA

Radionuclide scrotal imaging (RSI) has proven to be a valuable examination for patients with acute scrotal pain. It would be helpful to predict testicular viability using this method. We evaluated uptake of Tc-99m pertechnetate in the testis (T) and dartos (D) and correlated this with surgical and pathological findings.

48 RSI were performed in 46 patients (age 12-48) with acute scrotal pain. In tissue-phase RSI images, activity in T and D was recorded on a scale of 0 to 3: "0" representing activity equal to the opposite normal testis; "-1" < normal testis, but > that of thigh; "-2" = thigh; and "-3" < thigh. For activity in D, "0" = normal, "+1" = mildly increased, "+2" = that of femoral artery, and "+3" > that of femoral artery.

Decreased T activity ("-1" to "-3") was noted in all phases of torsion: early (< 7hr. after pain onset), middle (7-24 hr), and late (>24 hr.). When T activity was "-1", 57% (12/21) of the testes were viable, while 59% (13/22) of testes were viable when T was "-2" (P = N.S.). Activity in D, however, was "0" in early-phase torsion and increased to "+2 " or "+3" in late-phase torsion. The greater the activity in D, the lower the chance that the testicle could be saved. Salvageability was 94% (17/18) when D was "0", and 67% (6/9) when D was "+1." Only 9.5% (2/21) of the testes were salvaged when D activity was "+2" or greater.

In conclusion, dartos activity in tissue phase images of RSI is a reliable indicator for predicting testicular viability. This finding may be helpful in planning possible surgical intervention in patients with acute scrotal pain.